

---

## Two-Dimensional Problems of Electrohydrostatic Stability

D. H. Michael and M. E. O'Neill

*Phil. Trans. R. Soc. Lond. A* 1972 **272**, 331-359

doi: 10.1098/rsta.1972.0053

---

### Email alerting service

Receive free email alerts when new articles cite this article - sign up in the box at the top right-hand corner of the article or click [here](#)

---

To subscribe to *Phil. Trans. R. Soc. Lond. A* go to: <http://rsta.royalsocietypublishing.org/subscriptions>

---

# TWO-DIMENSIONAL PROBLEMS OF ELECTROHYDROSTATIC STABILITY

BY D. H. MICHAEL

*Department of Mathematics, University College London, England*

AND M. E. O'NEILL†

*Department of Chemical Engineering, Carnegie-Mellon University,  
Pittsburgh, Pennsylvania U.S.A.*

(Communicated by Sir Geoffrey Taylor, F.R.S. – Received 8 November 1971)

CONTENTS		PAGE
INTRODUCTION		332
1. A FORMULATION WHEN CHARGED FLUID SURFACES ARE CLOSE TOGETHER		332
Solutions of the equilibrium equation when $\alpha = 0$		334
Solutions of the equilibrium equation when $\alpha \neq 0$		335
2. SOME CONNECTED PROBLEMS		336
(a) Differing values of $\alpha$ and $\beta$ at the two surfaces		337
(b) One rigid surface		338
(c) Differing values of $a$ at the two surfaces		338
Solutions when $\alpha = 0$		339
Solutions when $\alpha \neq 0$		341
(d) One fixed surface when $a_1 \neq a_2$		343
3. A FORMULATION WHEN THE GAP BETWEEN THE FLUID SURFACES IS NOT NECESSARILY SMALL		343
Solutions when $\alpha = 0$		345
Solutions when $\alpha \neq 0$		346
Solutions when one surface is a rigid plane		348
4. A NUMERICAL STUDY OF A GENERAL TWO-DIMENSIONAL SURFACE EQUILIBRIUM PROBLEM		348
The numerical solution		351
A comparison between results from the exact and asymptotic theories		355
Some related problems		357
REFERENCES		359

The main intention of this paper is to study the breakdown of equilibrium of a conducting fluid surface such as a membrane when placed in the field of a charged cylindrical conductor. The work is presented in four sections. The first section outlines an approximate theory relevant when the gap between the cylinder and surface is small in comparison with the radius of the cylinder. In the second section, this theory is applied to a number of related problems notably the stability of conducting fluid filaments suspended on parallel wires. In the third section we introduce an extension of the asymptotic analysis of the preceding sections which removes the restriction of the small gap requirement and may be applied to

† Present address: Department of Mathematics, University College London, England.

problems of section two which possess symmetry about a centre plane. In the final section, we present a global analysis of the stability of a membrane in the field of a cylindrical conductor. Here the problem is studied in general terms without restrictions on geometrical parameters, and the resulting general equations determining the equilibrium configuration of the membrane are solved numerically.

### INTRODUCTION

A problem of interest in many areas of chemical engineering and in meteorology is the failure of the stability of equilibrium of two neighbouring bodies when electrified, leading often to their coalescence in the case of deformable and miscible bodies. The linearized theory of the instability of a single charged spherical drop was given by Rayleigh (1882). Taylor (1964) showed the existence of unstable equilibrium configurations of a single charged drop in a shape very closely spheroidal. He also deduced a criterion for instability of an uncharged drop in an external electric field, which is closely supported by experimental evidence. The effect of electric fields on the coalescence of water droplets with a plane water surface was studied by Jayaratne & Mason (1964), and the effect of electrostatic forces on the equilibrium and stability of two neighbouring drops has been studied by a number of authors, including Allan & Mason (1961, 1962), and Latham & Roxburgh (1966). An interesting experimental and theoretical study was carried out by Taylor (1968) into the equilibrium of two neighbouring drops or membranes, suspended on similarly situated parallel circular rings, when stressed by an electrostatic field. Further studies of the solutions of Taylor's equilibrium equation have been reported by Ackerberg (1969).

The main intention of this paper is to study the breakdown of equilibrium of a fluid surface such as a conducting membrane when placed in the field of a charged circular cylindrical conductor. The work is presented in four sections. The investigations reported in §§ 1 and 2 were suggested by the work of Taylor and Ackerberg and are relevant to the main problem when the gap between the cylinder and the surface is small in comparison with the radius of the cylinder. Here we may employ a two-dimensional analogue of the analysis presented by Taylor in the axisymmetric problem to give predictions of the breakdown potential. In § 3 we introduce an extension of the asymptotic analysis used in the preceding sections which removes the restriction of the small gap approximation. Apart from one case considered this improved asymptotic analysis does not appear to be applicable to systems where there is asymmetry about a centre plane, so we have been unable to apply the analysis to the main problem when the gap is finite. The paper concludes with § 4 in which a global analysis of the problem in general terms and without restrictions on geometrical parameters is set out. The general equations determining the equilibrium are presented and numerical solutions have been determined. We compare the results of the complete analysis with those obtained using the asymptotic analysis of the first section.

#### 1. A FORMULATION WHEN CHARGED FLUID SURFACES ARE CLOSE TOGETHER

We begin by considering the two-dimensional form of the problem studied by Taylor and Ackerberg. Two plane drops or membranes, suspended on two pairs of parallel wires AB and CD, as illustrated in figure 1 are similarly situated with  $AC = BD = 2h$  and  $AB = CD = 2a$ . The method employed by Taylor enables the stability of the equilibrium to be studied as a two-point boundary-value problem when  $h \ll a \ll R$ , where  $R$  denotes the radius of curvature of the surfaces. In these circumstances a good approximation to the electrostatic field can be obtained by

regarding the surfaces as parallel planes with the local distance between them. Thus if the potentials of AB and CD are taken as  $+V_0$  and  $-V_0$  respectively with  $V_0 > 0$  and axes  $Ox, Oy$  are taken as shown,  $Ox$  being in the central plane, the electric field is given by  $-V_0 \hat{j}/y(x)$ , where  $y = y(x)$  is the equation of the upper surface. Consequently the electrostatic stress on the surface is  $V_0^2/8\pi y^2$  in Gaussian units. Now assuming that  $h \ll a \ll R$ , it follows that  $x/a \approx 1$ ,  $y/h \approx 1$ ,

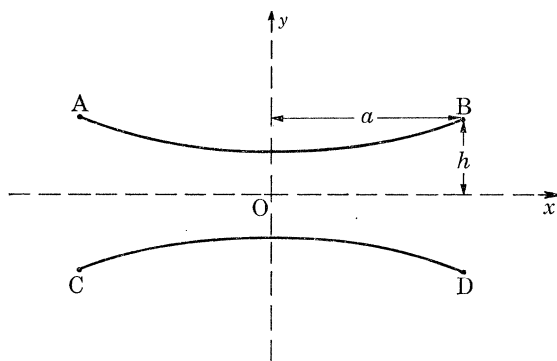


FIGURE 1. The arrangement of the conducting surfaces where there is symmetry about the midplane and  $h/a \ll 1$ .

$dy/dx \approx h/a \ll 1$  and the curvature of the surface may be written as  $d^2y/dx^2$  to the first order in  $h/a$ . The equation of equilibrium of the upper surface is then

$$T \frac{d^2y}{dx^2} - \frac{KV_0^2}{8\pi y^2} = p, \quad (1)$$

where, for drops,  $T$  is the surface tension,  $K$  is the dielectric constant of the medium exterior to the conducting surfaces and  $p$  is the excess of the internal static pressure of either drop over the external pressure. If we assume that  $p$  is unaffected by the application of the electric field, the value of  $p$  can then be related to the radius  $R$  of the drop surface in the absence of the electric field. In fact  $p = T/R$ , so that equation (1) may be written as

$$T \frac{d^2y}{dx^2} - \frac{KV_0^2}{8\pi y^2} = \frac{T}{R}.$$

When the fluid surfaces are membranes we must write  $2T$  for  $T$  in this equation. We now make  $x$  and  $y$  dimensionless with reference to  $a$  and  $h$  respectively. The equation of equilibrium then becomes

$$\frac{d^2y}{dx^2} = \alpha + \frac{\beta}{y^2}, \quad (2)$$

where  $\alpha = a^2/Rh$  and  $\beta = KV_0^2 a^2/8\pi Th^3$ .

Our method is then to look for solutions of (2) subject to the conditions  $dy/dx = 0$  at  $x = 0$  and  $y = 1$  at  $x = 1$ . It will be shown that this two point boundary-value problem yields an equilibrium solution provided that  $\beta$  lies below a critical value  $\beta_c$  which represents the limiting potential above which an equilibrium configuration of the surfaces does not exist.

We also note here that equation (1) represents a condition of stationary potential energy  $W$  where

$$W = \int_0^a \left\{ T \left[ 1 + \left( \frac{dy}{dx} \right)^2 \right]^{\frac{1}{2}} - \frac{KV_0^2}{8\pi y} + py \right\} dx.$$

If we let  $y$  be changed smoothly to  $y + \Delta y$  for  $x$  within the range  $(0, a)$  subject only to the preservation of the end conditions  $d(y + \Delta y)/dx = 0$  at  $x = 0$  and  $y + \Delta y = h$  at  $x = a$ , so that  $d(\Delta y)/dx = 0$  at  $x = 0$  and  $\Delta y = 0$  at  $x = a$ , it follows that

$$\begin{aligned} \delta W = & \int_0^a \left\{ -T \frac{d^2 y}{dx^2} \left[ 1 + \left( \frac{dy}{dx} \right)^2 \right]^{-\frac{3}{2}} + \frac{KV_0^2}{8\pi y^2} + p \right\} \Delta y \, dx \\ & + \int_0^a \left\{ \frac{T}{2} \left[ \frac{d\Delta y}{dx} \right]^2 \left[ 1 + \left( \frac{dy}{dx} \right)^2 \right]^{-\frac{3}{2}} - \frac{KV_0^2}{8\pi y^3} (\Delta y)^2 \right\} dx \\ & + \text{terms of order } (\Delta y)^3 \text{ and higher powers.} \end{aligned} \quad (3)$$

Equilibrium requires that  $W$  be stationary to the displacement, so that the first term in this expression yields the equilibrium equation which reduces to (1) in our approximation.

*Solutions of the equilibrium equation when  $\alpha = 0$*

When  $\alpha = 0$  it means that  $R = \infty$  and therefore the surfaces are initially plane before the application of the electric field. This may apply to drops or to membranes such as soap films suspended between the wires. For the latter it must be remembered that the surface tension is doubled. Setting  $\alpha = 0$  makes equation (2) immediately integrable. A first integral is

$$\left( \frac{dy}{dx} \right)^2 = 2\beta \left( \frac{1}{y_0} - \frac{1}{y} \right),$$

where  $y_0 \leq y \leq 1$  and  $y_0$  denotes the value of  $y$  when  $x = 0$ . If we write  $\xi = y/y_0$  ( $\xi \geq 1$ ) the second integration, together with the boundary condition at  $x = 1$ , yields

$$\xi^{\frac{1}{2}}(\xi - 1)^{\frac{1}{2}} + \sinh^{-1}(\xi - 1)^{\frac{1}{2}} - y_0^{-\frac{1}{2}}(y_0^{-1} - 1)^{\frac{1}{2}} - \sinh^{-1}(y_0^{-1} - 1)^{\frac{1}{2}} = (2\beta/y_0^3)^{\frac{1}{2}}(x - 1). \quad (4)$$

The boundary condition  $y = y_0$  at  $x = 0$  gives

$$y_0^{\frac{1}{2}}(1 - y_0)^{\frac{1}{2}} + y_0^{\frac{3}{2}} \sinh^{-1}(y_0^{-1} - 1)^{\frac{1}{2}} = (2\beta)^{\frac{1}{2}}, \quad (5)$$

which when used in (4) gives

$$\xi^{\frac{1}{2}}(\xi - 1)^{\frac{1}{2}} + \sinh^{-1}(\xi - 1)^{\frac{1}{2}} = (2\beta/y_0^3)^{\frac{1}{2}} x.$$

The equilibrium profile of the surface as determined here is shown in figure 2 for different values of  $\beta$  and the variation of  $\beta$  with  $y_0$ , deduced from (5), is illustrated in figure 3. As in the axisymmetric analysis it is seen that a maximum value of  $\beta$  exists; its value is  $\beta_c = 0.350$  and it occurs when  $y_0 = 0.617$ . We shall refer to this as a critical value, above which equilibrium configurations do not exist. As  $\beta$  is increased from zero it may be inferred from figures 2 and 3 that stable equilibrium configurations occur in the range  $1 > y_0 > 0.617$  and for values of  $y_0$  less than 0.617 the equilibrium is unstable. That such a transition in stability occurs at the maximum point of the  $(y_0, \beta)$  curve can be demonstrated as follows. If  $W(y_0, \beta)$  is the value of  $W$  for any point on this curve, we may treat this as a function of two independent variables on the understanding that an increment  $\delta y_0$  in  $y_0$  produces a change  $\Delta y(x)$  associated with a change to the neighbouring point  $(y_0 + \delta y_0, \beta + \delta \beta)$  on the curve. We then have  $\partial W / \partial y_0 = 0$  at each point of the curve since each is an equilibrium point. At the point of maximum  $\beta$  there are neighbouring points  $(y_0, \beta_c)$  and  $(y_0 + \delta y_0, \beta_c)$  at which  $\partial W / \partial y_0 = 0$ . Thus  $\partial^2 W / \partial y_0^2 = 0$  at this point. This implies that the second term of  $\delta W$  in (3) is also zero when  $y(x)$  is the solution at  $\beta = \beta_c$  and  $\Delta y$  is a change associated with a change  $\delta y_0$  from this point. Therefore  $\delta W$  is in general  $O(\delta y_0^3)$  at the maximum point, hence  $\delta W$  will change sign with a reversal in the sign of  $\delta y_0$ , thus showing that

the equilibrium becomes unstable at this point. Such a critical condition is analogous to the 'snapping' condition of elastic stability theory. For a more detailed discussion of such a condition the reader is referred to Thompson (1963).

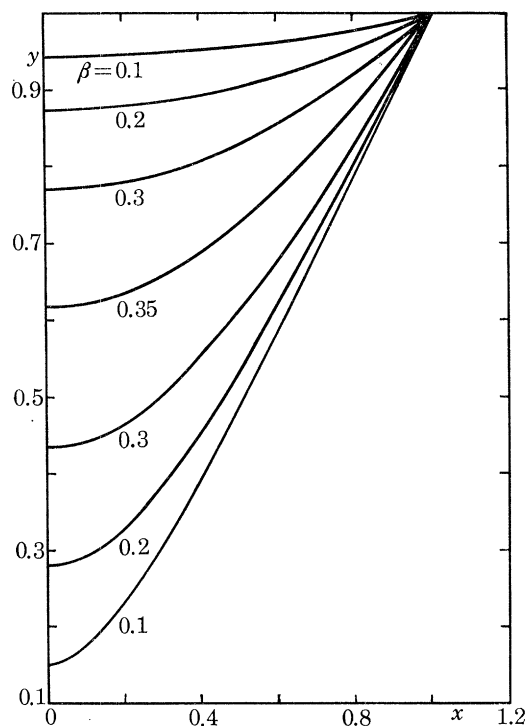


FIGURE 2. The profiles of the equilibrium shape of the upper half surface for different values of  $\beta$ .

*Solutions of the equilibrium equation when  $\alpha \neq 0$*

When  $\alpha \neq 0$  it is still possible to obtain solutions of equation (2) in closed form. The first integral of (2) gives

$$\left(\frac{dy}{dx}\right)^2 = \frac{2}{yy_0}(y-y_0)(\alpha yy_0 + \beta),$$

which satisfies the condition  $dy/dx = 0$  at  $x = 0$ . The second integral is then

$$\int_{y_0}^y \frac{y^{\frac{1}{2}} dy}{\{(y-y_0)(y+\beta/\alpha y_0)\}^{\frac{1}{2}}} = (2\alpha)^{\frac{1}{2}} x. \quad (6)$$

The left-hand side is expressible in terms of elliptic integrals of the first and second kinds on making the substitution  $y = y_0 \sec^2 \phi$ . This leads to

$$x = \left[ \frac{2(y_0/\alpha)}{1 + \beta/\alpha y_0^2} \right]^{\frac{1}{2}} \left\{ F(\phi, k) - \frac{E(\phi, k)}{1-k^2} + \frac{\tan \phi}{1-k^2} (1-k^2 \sin^2 \phi)^{\frac{1}{2}} \right\}, \quad (7)$$

where

$$k^2 = (\beta/\alpha y_0^2) (1 + \beta/\alpha y_0^2)^{-1}$$

and

$$E(\phi, k) = \int_0^\phi (1 - k^2 \sin^2 \phi)^{\frac{1}{2}} d\phi,$$

$$F(\phi, k) = \int_0^\phi (1 - k^2 \sin^2 \phi)^{-\frac{1}{2}} d\phi.$$

When  $x = 1, y = 1$  so that  $\phi = \phi_1$  where  $\sec^2 \phi_1 = 1/y_0$ . Hence

$$1 = \left[ \frac{2(y_0/\alpha)}{1 + \beta/\alpha y_0^2} \right]^{\frac{1}{2}} \left\{ F(\phi_1, k) - \frac{E(\phi_1, k)}{1-k^2} + \frac{\tan \phi_1}{1-k^2} (1-k^2 \sin^2 \phi_1)^{\frac{1}{2}} \right\}. \quad (8)$$

This equation gives the relation between  $\beta$  and  $y_0$  when  $\alpha \neq 0$  and in figure 3 we have plotted  $\beta$  as a function of  $y_0$  from equation (8) for  $\alpha = 0.25, 0.5, 1.0$ . It is easily verified from equation (2) that  $y_0 = 1 - \frac{1}{2}\alpha$  is the upper limit of  $y_0$  when  $\beta = 0$ . It is also a feature of the plane solution, which differs from the axisymmetric solution of Ackerberg (1969), that  $\beta \rightarrow 0$  as  $y_0 \rightarrow 0$ . The limiting solution in this case can be found by assuming that  $\beta/\alpha y_0$  has a finite limit as  $y_0 \rightarrow 0$  in equation (6), in which case

$$\int_0^y \frac{dy}{(y + \beta/\alpha y_0)^{\frac{1}{2}}} = (2\alpha)^{\frac{1}{2}} x.$$

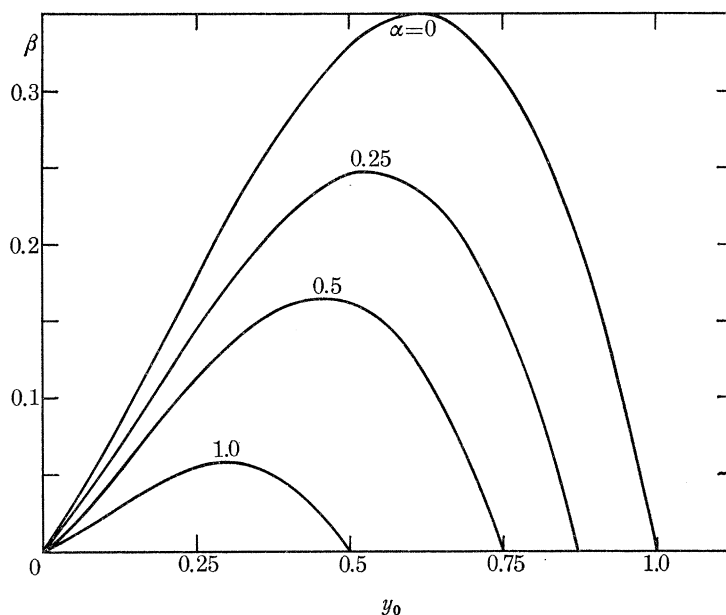


FIGURE 3. The variations of  $\beta$  with  $y_0$  for the fixed values of  $\alpha$ .

Using the boundary condition  $x = y = 1$ , we deduce that in the limit  $y_0 \rightarrow 0$ ,

$$\frac{\beta}{\alpha y_0} = \frac{1}{4} \left\{ \left( \frac{2}{\alpha} \right)^{\frac{1}{2}} - \left( \frac{2}{\alpha} \right)^{-\frac{1}{2}} \right\}^2.$$

The corresponding limiting form of the equilibrium surface is given by

$$\left( y + \frac{\beta}{\alpha y_0} \right)^{\frac{1}{2}} - \left( \frac{\beta}{\alpha y_0} \right)^{\frac{1}{2}} = \left( \frac{\alpha}{2} \right)^{\frac{1}{2}} x.$$

The general shapes of the loading curves in the  $(\beta, y_0)$  plane when  $\alpha \neq 0$  are similar to the curve for  $\alpha = 0$  and the discussion of the stability of the equilibrium configurations follows that already given for  $\alpha = 0$  and will not be repeated here.

## 2. SOME CONNECTED PROBLEMS

In this section we enumerate several problems which are similar to that discussed in § 1. We shall show that each of these problems can be reduced to the same type of boundary-value problem.

(a) Differing values of  $\alpha$  and  $\beta$  at the two surfaces

The value of  $\alpha$  is a measure of the equilibrium radius  $R$  or the volume of the drop on each side in the absence of the electric field. When the drops have different values of  $R$ , the values of  $\alpha$  associated with the drops are not equal and the geometrical symmetry about the mid-plane is lost. Similarly, if the surface tension is different at the surfaces, this gives rise to different values of  $\beta$  and a similar loss of symmetry. We may analyse these two effects together, using a notation which is indicated in figure 4 with the  $x$ -axis taken in CD. Let the upper and lower surfaces have equations  $y = y_1$  and  $y = y_2$  respectively and let the suffix 1 or 2 apply to a parameter associated with the upper or lower surface respectively.

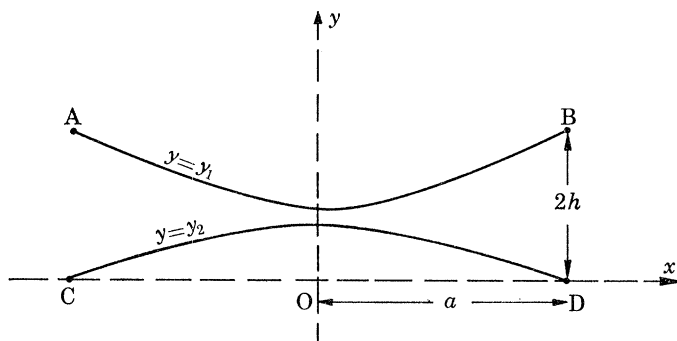


FIGURE 4. The arrangement of the conducting surfaces when there is asymmetry about the mid-plane.

The equations of equilibrium are now

$$T_1 \frac{d^2 y_1}{dx^2} = \frac{KV_0^2}{2\pi(y_1 - y_2)^2} + p_1, \quad T_2 \frac{d^2 y_2}{dx^2} = -\frac{KV_0^2}{2\pi(y_1 - y_2)^2} - p_2.$$

As in § 1 we again take the potentials of the upper and lower surfaces to be  $V_0$  and  $-V_0$  and we shall again assume that  $h \ll a \ll R$ . Now  $p_1 = T_1/R_1$ ,  $p_2 = T_2/R_2$  and if we regard  $x$  and  $y$  as dimensionless with reference to  $a$  and  $2h$  respectively, the dimensionless forms of the above differential equations are

$$\frac{d^2 y_1}{dx^2} = \alpha_1 + \frac{\beta_1}{(y_1 - y_2)^2}, \quad \frac{d^2 y_2}{dx^2} = -\alpha_2 - \frac{\beta_2}{(y_1 - y_2)^2}, \quad (9)$$

where

$$\alpha_1 = a^2/2hR_1, \quad \alpha_2 = a^2/2hR_2, \quad \beta_1 = KV_0^2 a^2/16\pi T_1 h^3 \quad \text{and} \quad \beta_2 = KV_0^2 a^2/16\pi T_2 h^3.$$

The boundary conditions to be satisfied by the solutions of (9) are

$$\frac{dy_1}{dx} = \frac{dy_2}{dx} = 0 \quad (x = 0), \quad y_1 = 1, y_2 = 0 \quad (x = 1).$$

Writing  $\xi = \beta_2 y_1 + \beta_1 y_2$ ,  $\eta = y_1 - y_2$ , the problem can be restated as

$$\frac{d^2 \xi}{dx^2} = \alpha_1 \beta_2 - \alpha_2 \beta_1, \quad \frac{d^2 \eta}{dx^2} = (\alpha_1 + \alpha_2) + \frac{\beta_1 + \beta_2}{\eta^2}, \quad (10)$$

with the boundary conditions  $d\xi/dx = d\eta/dx = 0$  at  $x = 0$  and  $\xi = \beta_2$ ,  $\eta = 1$  at  $x = 1$ .

The solution for  $\xi$  is clearly trivial and the characteristic value problem resides in the solution for  $\eta$ . This is evidently the same as that solved in § 1 with now  $\alpha$  and  $\beta$  replaced by  $\alpha_1 + \alpha_2$  and  $\beta_1 + \beta_2$  respectively.



(b) *One rigid surface*

Consider now the case when one of the conducting surfaces, the upper one for instance, is a fixed rigid surface. In the notation of (a) above, the problem reduces to solving the equation

$$T_2 \frac{d^2 y_2}{dx^2} = -\frac{KV_0^2}{2\pi(y_1 - y_2)^2} - \rho_2, \quad (11)$$

with  $dy_2/dx = 0$  at  $x = 0$  and  $y_2 = 1$  at  $x = 1$ . The function  $y_1$  now appears in (11) with a prescribed form. In the case when the upper surface is a circular cylinder of radius  $R_1$ , we have in this approximation

$$\frac{d^2 y_1}{dx^2} = \frac{a^2}{2hR_1},$$

and since  $y_1 = 1$  when  $x = 0$ , the approximate form for  $y_1$  is therefore  $y_1 = 1 - a^2(1 - x^2)/4hR_1$ . Clearly we should rewrite equation (11) with  $\eta$  as the dependent variable; the problem then reduces to the solution of

$$\frac{d^2 \eta}{dx^2} = \alpha^* + \frac{\beta^*}{\eta^2},$$

with  $\alpha^* = a^2(R_1^{-1} + R_2^{-1})/2h$  and  $\beta^* = KV_0^2 a^2/16\pi T_2 h^3$ , subject to the boundary conditions  $d\eta/dx = 0$  at  $x = 0$  and  $\eta = 1$  at  $x = 1$ . The problem is thus equivalent to that of § 1.

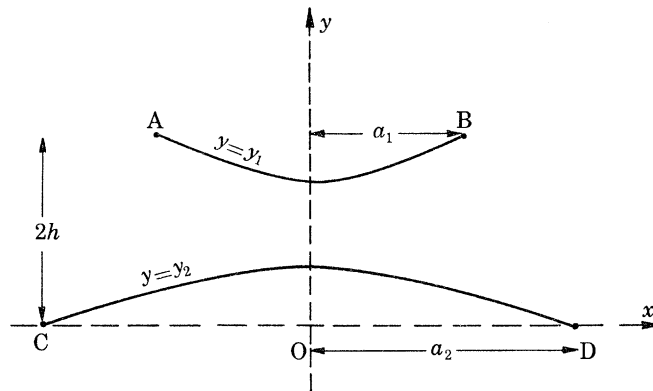


FIGURE 5. The arrangement of the conducting surfaces when  $a_1 \neq a_2$ .

(c) *Differing values of a at the two surfaces*

When the pairs of wires AB, CD are at different distances apart so that  $AB = 2a_1$ , and  $CD = 2a_2$ , we adopt a notation as indicated in figure 5. If we suppose that  $a_2 > a_1$ , then  $\sigma = a_2/a_1 > 1$ . With  $h \ll a_1$ , we may again use the same simplifying approximations with regard to curvature and electric field as in previous examples, but here we must make a further assumption concerning the end effects at  $x = a_1$ . A full treatment of this problem is to be obtained by taking into account the changes in the electric field which occur on the length scale  $2h$  in the neighbourhood of  $x = a_1$ . Here we shall neglect these effects and obtain a first approximation to the solution by assuming that the electrical stress on the lower surface is reduced to zero when  $x > a_1$ . This in effect means that we are replacing a transition in the value of  $d^2 y_2/dx^2$  on a length scale  $h$  by a finite discontinuity in this quantity.

Solutions when  $\alpha = 0$

When there is no excess pressure across the conducting surfaces the equations of equilibrium become

$$\begin{aligned} T \frac{d^2 y_1}{dx^2} - \frac{KV_0^2}{2\pi(y_1 - y_2)^2} &= 0 \quad (0 < x < a_1), \\ T \frac{d^2 y_2}{dx^2} + \frac{KV_0^2}{2\pi(y_1 - y_2)^2} &= 0 \quad (0 < x < a_1), \\ \frac{d^2 y_2}{dx^2} &= 0 \quad (a_1 < x < a_2). \end{aligned}$$

Here we assume that the surface tensions are the same at the two surfaces. The boundary conditions are

$$\begin{aligned} \frac{dy_1}{dx} = \frac{dy_2}{dx} &= 0 \quad (x = 0), \\ y_1 = 2h \quad (x = a_1), \quad y_2 &= 0 \quad (x = a_2), \end{aligned}$$

together with the requirement that  $y_2$  and  $dy_2/dx$  be continuous at  $x = a_1$ . In dimensionless form, with  $a_1$  used as the scale for  $x$  and  $2h$  as the scale for  $y$ , the equations become

$$\begin{aligned} \frac{d^2 y_1}{dx^2} - \frac{\beta}{(y_1 - y_2)^2} &= 0 \quad (0 < x < 1), \\ \frac{d^2 y_2}{dx^2} + \frac{\beta}{(y_1 - y_2)^2} &= 0 \quad (0 < x < 1), \\ \frac{d^2 y_2}{dx^2} &= 0 \quad (1 < x < \sigma), \end{aligned}$$

with  $\beta = KV_0^2 a_1^2 / 16\pi T h^3$ . The boundary conditions require  $y_1 = 1$  at  $x = 1$ ,  $y_2 = 0$  at  $x = \sigma$  and  $y_2$ ,  $dy_2/dx$  to be continuous at  $x = 1$ . Clearly  $y_2 = \lambda(x - \sigma)$  for  $1 < x < \sigma$ , where  $\lambda$  is a constant. Consequently  $y_2 = \lambda(1 - \sigma)$  and  $dy_2/dx = \lambda$  at  $x = 1$ . Hence the boundary condition which the solution for  $y_2$  for  $0 < x < 1$  must satisfy at  $x = 1$  is

$$(1 - \sigma) (dy_2/dx) - y_2 = 0.$$

We can again simplify the determination of  $y_1$  and  $y_2$  by writing  $\xi = y_1 + y_2$ ,  $\eta = y_1 - y_2$  for  $0 < x < 1$ . The equations for  $\xi$  and  $\eta$  are

$$\frac{d^2 \xi}{dx^2} = 0, \quad \frac{d^2 \eta}{dx^2} - \frac{2\beta}{\eta^2} = 0. \quad (12)$$

At  $x = 0$ ,  $d\xi/dx = d\eta/dx = 0$ , so that  $\xi = \text{constant}$  for all  $x$  such that  $0 < x < 1$ . Hence

$$dy_2/dx = -dy_1/dx$$

in this range and  $d\eta/dx = -2dy_2/dx$ . Thus at  $x = 1$  we have  $\xi = 1 + y_2$ ,  $\eta = 1 - y_2$ ,  $d\xi/dx = 0$  and  $d\eta/dx = -2y_2/(1 - \sigma)$ . Hence the boundary condition on  $\eta$  at  $x = 1$  is

$$(\sigma - 1) (d\eta/dx) + 2\eta = 2. \quad (13)$$

With  $\beta^* = 2\beta$ , the solution of (12) with  $d\eta/dx = 0$  at  $x = 0$  follows immediately from § 1. If we write  $\zeta = \eta/\eta_0$  where  $\eta = \eta_0$  at  $x = 0$ , we have from equation (4)

$$\zeta^{\frac{1}{2}} (\zeta - 1)^{\frac{1}{2}} + \sinh^{-1} (\zeta - 1)^{\frac{1}{2}} = (2\beta^*/\eta_0^3)^{\frac{1}{2}} x + \text{const.}, \quad (14)$$

and the constant is such as to satisfy condition (13) at  $x = 1$ . If we denote by  $\zeta_1$  the value of  $\zeta$  at  $x = 1$ , this condition is

$$(\sigma - 1) \left( \frac{2\beta^*}{\eta_0^3} \right)^{\frac{1}{2}} \left( \frac{\zeta_1 - 1}{\zeta_1} \right)^{\frac{1}{2}} = 2 \left( \frac{1}{\eta_0} - \zeta_1 \right). \quad (15)$$

Equation (14) may also be written as

$$\zeta^{\frac{1}{2}}(\zeta - 1)^{\frac{1}{2}} + \sinh^{-1}(\zeta - 1)^{\frac{1}{2}} - \left\{ \zeta_1^{\frac{1}{2}}(\zeta_1 - 1)^{\frac{1}{2}} + \sinh^{-1}(\zeta_1 - 1)^{\frac{1}{2}} \right\} = (2\beta^*/\eta_0^3)(x - 1),$$

and since  $\zeta = 1$  when  $x = 0$ ,

$$(2\beta^*/\eta_0^3)^{\frac{1}{2}} = \zeta_1^{\frac{1}{2}}(\zeta_1 - 1)^{\frac{1}{2}} + \sinh^{-1}(\zeta_1 - 1)^{\frac{1}{2}}. \quad (16)$$

Writing (15) in the form

$$\frac{1}{\eta_0} = \zeta_1 + \frac{1}{2}(\sigma - 1) \left( \frac{2\beta^*}{\eta_0^3} \right)^{\frac{1}{2}} \left( 1 - \frac{1}{\zeta_1} \right)^{\frac{1}{2}}, \quad (17)$$

we may regard (16) and (17) as parametric equations for  $\beta^*$  and  $\eta_0$  with parameter  $\zeta_1$  where  $1 < \zeta_1 < \infty$ . When  $\zeta_1 = 1$ ,  $\eta_1 = \eta_0 = 1$  and  $\beta^* = 0$ . This is the case when there is no electric field and  $y_0 = 0$ ,  $y_1 = 1$ . The other limit is when  $\zeta_1 \rightarrow \infty$  which occurs when  $\eta_0 \rightarrow 0$ . From (17) we see that  $(2\beta^*/\eta_0^3) \rightarrow \infty$  like  $\zeta_1^2$ . But  $\zeta_1 \approx 1/\eta_0$ , hence  $\beta^* = O(\eta_0)$  as  $\eta_0 \rightarrow 0$ .

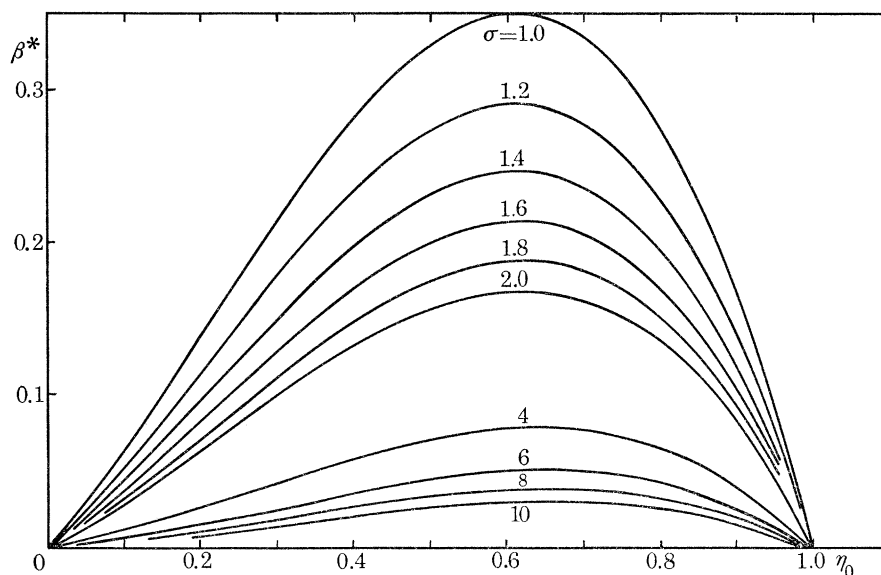


FIGURE 6. The variation of  $\beta^*$  with  $\eta_0$  for fixed values of  $\sigma$ .

For the purposes of computation it is desirable to write  $\zeta_1 = 1/z$  say in (16) and (17). This then reduces the range of the parameter to  $0 < z < 1$ . Figure 6 shows the variation of  $\beta^*$  with  $\eta_0$  for selected values of  $\sigma$ . Also included in this figure is the corresponding curve for  $\sigma = 1$  from § 1. In table 1 we list the values of  $\beta_c$  for the selected values of  $\sigma$ .

TABLE 1

$\sigma$	$\beta_c$	$\sigma$	$\beta_c$
1.0	0.350	2.0	0.168
1.2	0.291	4.0	0.0799
1.4	0.247	6.0	0.0520
1.6	0.215	8.0	0.0385
1.8	0.190	10.0	0.0306

*Solutions when  $\alpha \neq 0$*

We shall suppose that the surfaces have radii  $R_1$  and  $R_2$  when the electric field is zero. The equations in dimensionless form are then

$$\begin{aligned}\frac{d^2y_1}{dx^2} &= \alpha_1 + \frac{\beta}{(y_1 - y_2)^2} \quad (0 < x < 1), \\ \frac{d^2y_2}{dx^2} &= -\alpha_2 - \frac{\beta}{(y_1 - y_2)^2} \quad (0 < x < 1), \\ \frac{d^2y_2}{dx^2} &= -\alpha_2 \quad (1 < x < \sigma).\end{aligned}$$

Quantities appearing in the above equations are as defined for  $\alpha = 0$ . In addition, we have  $\alpha_1 = a_1^2/2hR_1$  and  $\alpha_2 = a_2^2/2hR_2$ . We have again assumed that the surface tension is the same on the two surfaces. The boundary conditions remain as for  $\alpha = 0$ . When  $1 < x < \sigma$  the solution for  $y_2$  is given by

$$y_2 = -\frac{1}{2}\alpha_2(x^2 - \sigma^2) + c(x - \sigma),$$

where  $c$  is a constant of integration. On setting  $x = 1$  and eliminating  $c$ , we obtain the boundary condition which the solution for  $y_2$  in  $(0 < x < 1)$  must satisfy at  $x = 1$ . This condition is

$$(\sigma - 1) (dy_2/dx) + y_2 = \frac{1}{2}\alpha_2(\sigma - 1)^2. \quad (18)$$

Proceeding as in the previous case, the equations to be solved are

$$\frac{d^2\xi}{dx^2} = \alpha_1 - \alpha_2, \quad \frac{d^2\eta}{dx^2} = \alpha_1 + \alpha_2 + \frac{2\beta}{\eta^2} \quad (0 < x < 1). \quad (19)$$

Hence  $d\xi/dx = (\alpha_1 - \alpha_2)x$ , from which we may deduce that  $d\eta/dx = \alpha_1 - \alpha_2 - 2dy_2/dx$  at  $x = 1$ . Substitution for  $dy_2/dx$  and  $y_2 = 1 - \eta$  in (18) yields

$$(\sigma - 1) (d\eta/dx) + 2\eta = (\alpha_1 - \alpha_2) (\sigma - 1) + 2 - \alpha_2(\sigma - 1)^2, \quad (20)$$

as the condition to be satisfied at  $x = 1$ . Writing  $\alpha^* = \alpha_1 + \alpha_2$ ,  $\beta^* = 2\beta$ , the solution of equation (19) satisfying the condition  $d\eta/dx = 0$  at  $x = 0$  we can quote from equation (7) as

$$x = \left[ \frac{2\eta_0/\alpha^*}{1 + \beta^*/\alpha^*\eta_0^2} \right]^{\frac{1}{2}} \left\{ F(\phi, k) - \frac{E(\phi, k)}{1 - k^2} + \frac{\tan \phi}{1 - k^2} (1 - k^2 \sin^2 \phi)^{\frac{1}{2}} \right\}, \quad (21)$$

where  $\eta = \eta_0 \sec^2 \phi$  and  $k^2 = (\beta^*/\alpha^*\eta_0^2) (1 + \beta^*/\alpha^*\eta_0^2)^{-1}$ . If  $\phi = \phi_1$  when  $x = 1$ , the boundary condition becomes

$$2(\sigma - 1) \eta_0 \sec^2 \phi_1 \tan \phi_1 [\partial\phi/\partial x]_{\phi_1} + 2\eta_0 \sec^2 \phi_1 - (\alpha_1 - \alpha_2) (\sigma - 1) + \alpha_2(\sigma - 1)^2 - 2 = 0. \quad (22)$$

We note here that the range of values of  $\alpha_1$  and  $\alpha_2$  are not unrestricted since when  $\beta = 0$ ,  $\eta = (y_1 - y_2) > 0$ . For  $\beta = 0$ ,

$$\begin{aligned}y_1 &= 1 + \frac{1}{2}\alpha_1(x^2 - 1) \quad (0 \leq x \leq 1), \\ y_2 &= \frac{1}{2}\alpha_2(\sigma^2 - x^2) \quad (0 \leq x \leq \sigma).\end{aligned}$$

Consequently  $\alpha_1 + \sigma^2\alpha_2 < 2$ . Numerical solutions of this boundary value problem have been obtained in the case when  $\alpha_1 = \alpha_2 = \alpha$ . There the range of permissible values of  $\alpha$  for a given value of  $\sigma$  is

$$0 < \alpha < 2(1 + \sigma^2)^{-1}.$$

Furthermore, when  $\beta = 0$ ,  $\eta_0 = 1 - \frac{1}{2}\alpha(1 + \sigma^2)$  and since the effect of increasing  $\beta$  from zero is to draw the surfaces together at  $x = 0$ , it follows that for any choice of  $\beta > 0$ ,

$$0 < \eta_0 < 1 - \frac{1}{2}\alpha(1 + \sigma^2).$$

The method by which we determined the values of  $\beta_c$  for given values of  $\sigma$  and  $\alpha$  (in the permitted range) was as follows. We first divided up the  $\eta_0$  range into fairly coarse subintervals (say 10) and proceeded to derive the value of  $\beta$  pertinent to the largest value of  $\eta_0$  less than its upper bound value. By choosing a small trial value of  $\beta$  we could then determine  $k$  and compute the solution of the equation (21) with  $x = 1$  by Newton's method. The left-hand side of (22) was then computed for the value of  $\phi_1$  now determined. If  $\beta$  is chosen sufficiently small this expression is negative and, by increasing  $\beta$ , the procedure can be repeated until the boundary condition (22) is satisfied to any prescribed degree of accuracy. In our calculations we aimed at satisfying the condition (22) to four decimal places. We would then know the values of  $\beta$  and  $\phi_1$  for the particular choice of  $\sigma$ ,  $\alpha$  and  $\eta_0$ . The complete calculation was then repeated for the smaller values of  $\eta_0$  in the set defined by the subdivision of the  $\eta_0$  range, the computations ceasing when the value of  $\beta$  for a particular  $\eta_0$  was less than that for the previous  $\eta_0$ ; this would indicate that we had passed beyond the maximum of the  $(\beta, y_0)$  curve. The value  $\beta_c$  of the maximum could then be determined as accurately as required (we worked to four decimal places) by increasing the number of subdivision points for  $\eta_0$  in the neighbourhood of the maximum. The results of these computations for  $\beta_c$  and  $\eta_0$  are displayed in table 2.

TABLE 2

$\sigma$	$\alpha$	$\eta_0$	$\beta_c$
1.1	0.0	0.6100	0.1589
	0.01	0.6063	0.1543
	0.1	0.5453	0.1167
	0.3	0.4045	0.0549
	0.4	0.3426	0.0341
	0.6	0.2005	0.0090
	0.8	0.0667	0.0005
1.2	0.0	0.6110	0.1453
	0.01	0.6049	0.1406
	0.1	0.5368	0.1025
	0.3	0.3836	0.0427
	0.4	0.3046	0.0240
	0.6	0.1541	0.0041
1.5	0.0	0.6175	0.1149
	0.01	0.6095	0.1095
	0.1	0.5063	0.0685
	0.3	0.2920	0.0158
	0.4	0.1803	0.0047
2.0	0.0	0.6250	0.0843
	0.01	0.6080	0.0774
	0.1	0.4350	0.0314
	0.3	0.0588	0.0002
5.0	0.0	0.6450	0.0315
	0.005	0.5750	0.0227
	0.01	0.5090	0.0157
	0.02	0.3700	0.0063
	0.03	0.2379	0.0002

There is a further variant of this problem, namely when the surface tensions at the surfaces are different, resulting in parameters  $\beta_1$  and  $\beta_2$  associated with the surfaces, with  $\beta_1 \neq \beta_2$ . The

technique of solution of this type of problem is essentially a combination of the methods used for problem (a) and the above problem, so we shall not elaborate further on this.

(d) *One fixed surface when  $a_1 \neq a_2$*

This example concludes our discussion of related problems in this section. We feature this case in particular because it has a special significance to the problem we shall discuss in § 4.

Referring again to figure 5, let us now suppose that the upper surface is a fixed circular cylinder of radius  $R_1$  so that

$$y_1 = 1 - a_1^2(1 - x^2)/4hR_1. \quad (23)$$

Using the same dimensionless quantities as before we find as in problem (b) above that

$$\frac{d^2\eta}{dx^2} = \alpha^* + \frac{\beta^*}{\eta^2} \quad (0 < x < 1), \quad (24)$$

where  $\alpha^* = \alpha_1 + \alpha_2$  with  $\alpha_1 = a_1^2/2hR_1$ ,  $\alpha_2 = a_2^2/2hR_2$  and  $\beta^* = KV_0^2 a_1^2/16\pi T_2 h^3$ . For  $1 < x < \sigma$  the analysis of (c) above may be applied to derive the boundary condition (18) for  $y_2$  at  $x = 1$ . By use of (23) we can convert this into a condition on  $\eta$  at  $x = 1$ , which is

$$(\sigma - 1) (d\eta/dx) + \eta = 1 + (\sigma - 1) \alpha_1 - \frac{1}{2}\alpha_2(\sigma - 1)^2. \quad (25)$$

Equations (24) and (25), together with the condition  $d\eta/dx = 0$  at  $x = 0$ , complete the specification of the boundary-value problem for this example.

The case when  $\alpha_2 = 0$  is of particular interest since this corresponds to a conducting surface which in the absence of the electric field would be plane. We are in a position to assess the accuracy of the predictions for  $\beta_c$  given by the asymptotic theory since in § 4 we show how the exact solution of a geometrically similar model may be determined numerically. We shall give the results of our calculations based on the theory developed here for  $\alpha_2 = 0$  in our discussion in § 4 but would point out here that the boundary-value problem is analogous to that of (c) and the solution for  $\beta_c$  for prescribed values of  $\alpha$  and  $\sigma$  may be found by the method outlined in our presentation for that problem. An alternative approach, and one which we in fact adopted here, would be to integrate equation (24) directly by a numerical method using the boundary condition  $d\eta/dx = 0$  at  $x = 0$  and a prescribed initial value for  $\eta$  at  $x = 0$ . The integration would first be carried out with a suitably chosen trial value of  $\beta$  and the integration procedure repeated with other values of  $\beta$  until the boundary condition (25) were satisfied to the required degree of accuracy. We used a fourth-order Runge–Kutta procedure for integration of (24) and refined the values of  $\beta$  to obtain satisfaction of (25) by using a linear interpolation–extrapolation formula.

In setting up the equations of equilibrium throughout this section we have assumed a droplet model. The only change that has to be made if the deformable conducting surfaces are membranes is to double the surface tension on each of the membrane surfaces. This would have no effect on the relations between the dimensionless parameters describing the equilibrium configuration. Hence all of the preceding results apply equally well to droplet and membrane surface models.

### 3. A FORMULATION WHEN THE GAP BETWEEN THE FLUID SURFACES IS NOT NECESSARILY SMALL

The axisymmetric analysis of Taylor and Ackerberg and the work on the two-dimensional problems of the previous sections are based on the assumption that  $h \ll a \ll R$ . This assumption leads to a simplified expression for the curvature and it enables us to make a simple approximation

to the electric field. When  $h/a \approx 1$  it is no great difficulty to take account of the curvature fully, but a better approximation to the field must be used in this case since the surfaces incur finite variations in their slopes. It appears to be a matter of some difficulty to simulate the field by a better approximation than that used in earlier work in general cases where there is asymmetry in the positions of the surfaces but when they are symmetrically situated relative to a centre plane, a fairly simple second approximation to the field may be found. Thus in a typical geometrical configuration depicted in figure 7 we approximate the electrostatic stress at a point on a fluid surface by means of the field within a wedge of angle  $2\psi$  where  $\tan \psi$  is the slope of the surface at the particular point, treating the surfaces as locally plane but with the correct local slope. If we take polar coordinates  $(r, \theta)$  with pole at the vertex of the wedge, the solution for the potential  $V$  within the wedge is

$$V = V_0 \theta / \psi,$$

where we again assume that the surfaces are at potentials  $\pm V_0$ . Thus the local electrostatic stress on either of the surfaces is

$$\frac{KV_0^2}{8\pi\psi^2 r^2} = \frac{KV_0^2 \sin^2 \psi}{8\pi y^2 \psi^2},$$

taken at the point of contact between the wedge and the surface. We note here the difficulty that arises in general when there is asymmetry about the midplane for in this case it is not known which wedge solution to adopt. The equation of equilibrium may now be written as

$$T \cos^3 \psi \frac{d^2 y}{dx^2} - \frac{KV_0^2 \sin^2 \psi}{8\pi y^2 \psi^2} = p, \quad (26)$$

where  $p = T/R$  is the excess pressure across the surface and  $R$  is the radius in the absence of the electric field.

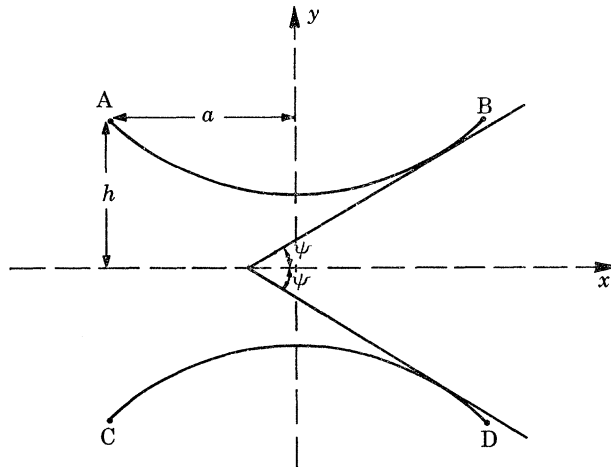


FIGURE 7. The arrangement of the conducting surfaces when there is symmetry about the mid-plane and  $h/a = O(1)$ .

Since  $h/a \approx 1$ , we now make both  $x$  and  $y$  dimensionless on the length scale  $a$ . Equation (26) then becomes in dimensionless form

$$\cos^3 \psi \frac{d^2 y}{dx^2} = \alpha + \frac{\beta \sin^2 \psi}{y^2}, \quad (27)$$

where  $\alpha = a/R$  and  $\beta = KV_0^2/8\pi a T$  from which it follows that  $0 \leq \alpha \leq 1$ . Equation (27) is to be solved subject to the boundary conditions  $dy/dx = 0$  at  $x = 0$  and  $y = s$  at  $x = 1$ , where  $s = h/a$ . Clearly the former condition is equivalent to  $\psi = 0$  when  $x = 0$ .

Solutions when  $\alpha = 0$

When there is no excess pressure across the fluid surface,  $\alpha = 0$  and (27) reduces to

$$\cos^3 \psi \frac{d^2 y}{dx^2} = \sin \psi \frac{d\psi}{dy} = \frac{\beta \sin^2 \psi}{y^2 \psi^2}. \quad (28)$$

A first integral of (28) is 
$$\beta \left( \frac{1}{y_0} - \frac{1}{y} \right) = \int_0^\psi \frac{\theta^2 d\theta}{\sin \theta}.$$

If we write  $z = 1/y$ ,  $z_0 = 1/y_0$ , the parametric equations for  $z$  and  $x$  in terms of the parameter  $\psi$  are

$$z = z_0 - \frac{1}{\beta} \int_0^\psi \frac{\theta^2 d\theta}{\sin \theta}, \quad (29)$$

$$x = \frac{1}{\beta} \int_0^\psi \frac{\theta^2 \cos \theta d\theta}{z^2 \sin^2 \theta}. \quad (30)$$

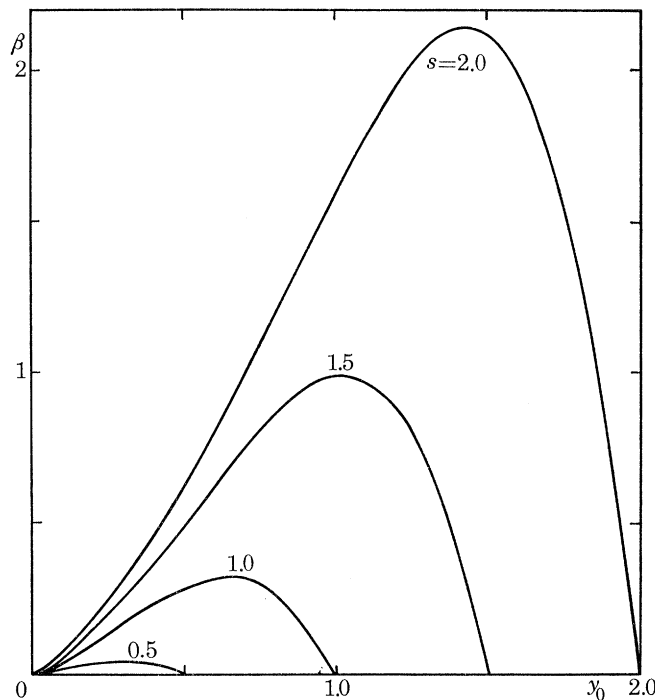


FIGURE 8. The variation of  $\beta$  with  $y_0$  for fixed values of  $s$  when  $\alpha = 0$ .

When  $\psi \ll 1$ , equations (29) and (30) should give asymptotically the solution derived in § 1. We observe that the asymptotic forms of (29) and (30) when  $\psi \ll 1$  are

$$z = z_0 - (\psi^2/2\beta), \quad (31)$$

and

$$x = \frac{1}{\sqrt{(2\beta z_0^3)}} \left\{ \frac{\sqrt{(2\beta z_0)} \psi}{2\beta z_0 - \psi^2} + \log \left[ \frac{\sqrt{(2\beta z_0)} + \psi}{\sqrt{(2\beta z_0 - \psi^2)}} \right] \right\}. \quad (32)$$

From (31),  $\psi = (2\beta z_0)^{\frac{1}{2}} (1 - y_0/y)^{\frac{1}{2}}$  and it easily follows that

$$\left( \frac{2\beta}{y_0^3} \right)^{\frac{1}{2}} x = \left( \frac{y}{y_0} \right)^{\frac{1}{2}} \left( \frac{y}{y_0} - 1 \right)^{\frac{1}{2}} + \sinh^{-1} \left( \frac{y}{y_0} - 1 \right)^{\frac{1}{2}}, \quad (33)$$



which agrees with the results of § 1. It should be noted, however, that there are differences in scaling in the way that the dimensionless parameters  $y$  and  $\beta$  are defined in this section as compared with the corresponding definitions given in § 1. If the bar denotes quantities of § 1, we have

$$\beta = s^3 \bar{\beta}, \quad y = s \bar{y}, \quad (34)$$

and since the scaling for  $x$  is the same throughout, it follows that (33) holds for both sets of parameters.

The critical values  $\beta_c$  of  $\beta$  for  $\psi = O(1)$  may be determined from (29) and (30) with the use of the condition  $z = 1/s$  when  $x = 1$ , but it is more convenient in practice to include the case  $\alpha = 0$  with the general case  $\alpha \neq 0$  for computational purposes. In figure 8 we display the  $(\beta, y_0)$  curves for a range of values of  $s$  for the case when  $\alpha = 0$  and in figure 9 the critical value  $\beta_c$  is plotted as a function of  $s$ .

#### *Solutions when $\alpha \neq 0$*

By noting that  $\tan \psi = dy/dx$ , it follows that the two point boundary-value problem set out above is equivalent to the first-order differential equation system

$$\frac{dy}{d\psi} = \frac{y^2 \psi^2 \sin \psi}{\alpha y^2 \psi^2 + \beta \sin^2 \psi}, \quad (35)$$

$$\frac{dx}{d\psi} = \frac{y^2 \psi^2 \cos \psi}{\alpha y^2 \psi^2 + \beta \sin^2 \psi}, \quad (36)$$

with  $x = 0$  when  $\psi = 0$  and  $y = s$  when  $\psi = \psi_1$ , the value  $\psi_1$  being such that  $x = 1$  when  $\psi = \psi_1$  ( $0 < \psi_1 < \frac{1}{2}\pi$ ). It has not proved possible to find the exact solutions of (35) and (36) apart from the particular case when  $\alpha = 0$  which has been discussed above. Numerical integration of the equations using the second order Runge–Kutta method has been carried out for  $\alpha = 0, 0.03125, 0.0625, 0.125, 0.25, 0.5, 0.75, 1.0$  and for each of these values of  $\alpha$ , selected values of  $s$  within the range  $(0.1, 2.0)$ . The lower bound of the range of permissible values of  $s$  for a given choice of  $\alpha$  is determined by the geometrical constraint

$$(R^2 - a^2)^{\frac{1}{2}} + sa \geq R,$$

from which it follows that for  $0 < \alpha \leq 1$

$$s \geq \frac{1}{\alpha} - \left( \frac{1}{\alpha^2} - 1 \right)^{\frac{1}{2}},$$

and when  $\alpha = 0, s > 0$ . The calculation of the critical value  $\beta_c$  for any given  $\alpha$  and  $s$  was carried out in the following manner. Since  $\psi < \frac{1}{2}\pi$  and the error in the integration method adopted is  $O(\delta^3)$  at each step, a value of the step length  $\delta = 10^{-3}\pi$  was chosen so that  $\beta_c$  could ultimately be determined to an accuracy of four decimal places. A value of  $y_0$  was prescribed for the initial value of  $y$  (at  $\psi = 0$ ) so that  $y_0 < s$ , and with a given value of  $\beta$ , equations (35) and (36) were integrated forward in turn until the value of  $x$  just exceeded 1. The value of  $\psi$  at which  $x = 1$  was deduced by interpolation and the value of  $y$  at this value of  $\psi$  was compared with  $s$ . If there was agreement to six decimal places the integration was terminated, otherwise the value of  $\beta$  was adjusted and the integration recommenced from  $\psi = 0$ . After two trial values of  $\beta$ , the refinement of the choice of  $\beta$  was then effected by the use of a linear interpolation–extrapolation formula relating the choice of  $\beta$  with the value of  $y$  when  $x = 1$ . In this way the value of  $\beta$  for which the differential equations (35) and (36) together with the boundary conditions has a solution for the given choice

of  $y_0$  could be determined. The value of  $y_0$  was then changed and the procedure started again. We could thus determine the variation of  $\beta$  with  $y_0$  for given values of  $\alpha$  and  $s$ , and  $\beta_c$ , the maximum value of  $\beta$ , could then be found.

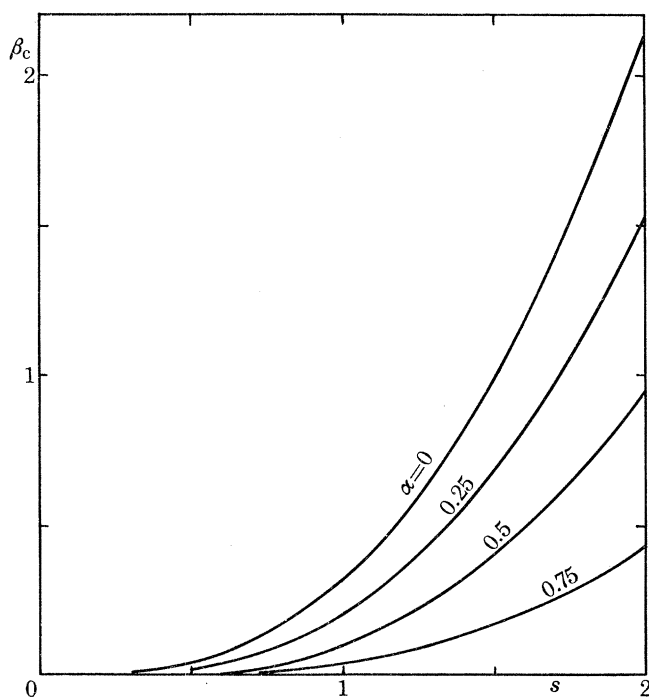


FIGURE 9. The variation of  $\beta_c$  with  $s$  for fixed values of  $\alpha$ .

In figure 9 the variation of  $\beta_c$  with  $s$  for different fixed values of  $\alpha$  is illustrated and in table 3 we compare the values of  $\beta_c$  for small values of  $s$  predicted by the asymptotic theories developed both in this section and in § 1. This is most conveniently accomplished by tabulating  $\beta_c$  and  $s^3\bar{\beta}_c$  for different values of  $\bar{\alpha}$  and  $s$ , where  $\bar{\alpha}$  and  $\bar{\beta}_c$  denote the values of  $\alpha$  and  $\beta_c$  of § 1. Consequently  $\bar{\beta}_c$  is a constant for each value of  $\bar{\alpha}$  and since the definitions of  $\alpha$  and  $\beta$  in this section are such that

$$\alpha = s\bar{\alpha}, \quad \beta = s^3\bar{\beta}_c,$$

it follows that for given values of  $\bar{\alpha}$  and  $s$ , the correct value of  $\beta_c$  is that evaluated for  $\alpha = s\bar{\alpha}$ .

TABLE 3

$\bar{\alpha}$	$s$	$\alpha = s\bar{\alpha}$	$s^3\bar{\beta}_c$	$\beta_c$
0.0	0.125	0.0	0.0007	0.0007
	0.25	0.0	0.0055	0.0055
	0.5	0.0	0.0438	0.0438
0.25	0.125	0.03125	0.0005	0.0005
	0.25	0.0625	0.0038	0.0038
	0.5	0.125	0.0307	0.0290
0.5	0.125	0.0625	0.0003	0.0003
	0.25	0.125	0.0026	0.0025
	0.5	0.25	0.0205	0.0180
1.0	0.125	0.125	0.0001	0.0001
	0.25	0.25	0.0009	0.0009
	0.5	0.5	0.0072	0.0045

Our numerical investigations thus show that for the chosen values of  $\bar{\alpha}$  there is a good measure of agreement for  $0 < s < 0.5$  between the values predicted by the theory of § 1 when we assume  $s \ll 1$  and the theory developed in this section where now we assume only that  $s = O(1)$ . It appears that for a given value of  $s$  the agreement between the theories improves as  $\bar{\alpha} \rightarrow 0$ .

*Solutions when one surface is a rigid plane*

We conclude this section by remarking that although the asymptotic method for determining  $\beta_c$  derived in this section appears to be unsuitable for general situations where there is asymmetry about the mid-plane between the conducting surfaces, there is however one example where the theory may be applied. This is when one of the surfaces is a rigid conducting plane. If we identify the conducting plane with the mid-plane of figure 7 and choose the deformable surface to be in the upper half-space, it follows that we can approximate the electrostatic stress at any point on the deformable surface by means of the field in a wedge of angle  $\psi$ , again treating the surface as locally plane but with the correct local slope  $\tan \psi$ . Consequently equation (27), and all the subsequent analysis, will apply to this problem as well, without change, if the plane is at zero potential. If the plane is at potential  $-V_0$ , the potential within the wedge is

$$V_0(\theta - \frac{1}{2}\psi)/\frac{1}{2}\psi,$$

so that the modified definition of  $\beta$  for equation (27) is  $\beta = KV_0^2/2\pi aT$ . In the foregoing discussions in this section we have assumed that the deformable bodies are drops. For a membrane it is again only necessary to write  $2T$  for  $T$  in the definition of  $\beta$ .

#### 4. A NUMERICAL STUDY OF A GENERAL TWO-DIMENSIONAL SURFACE EQUILIBRIUM PROBLEM

In this section we consider the equilibrium of an electrically conducting surface which in the absence of the electric field is plane and given by  $y = 0$ . We suppose that this surface consists of a long membrane of finite width  $2X$  attached along the lines  $x = \pm X$  to infinite rigid conducting half planes  $y = 0$ ,  $|x| > X$ . A rigid conducting circular cylinder of radius  $R$  is placed symmetrically with its axis at a distance  $H$  from the fluid-solid surface. The potential of the cylinder

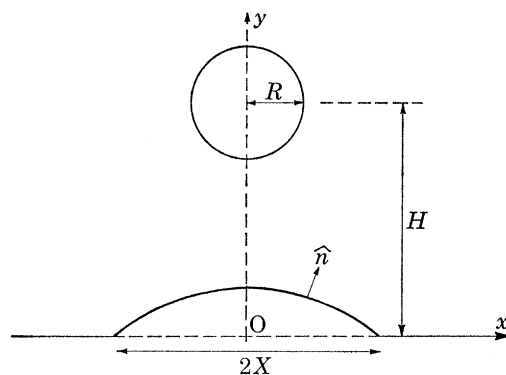


FIGURE 10. The arrangement of the cylinder and membrane in a typical equilibrium configuration.

is now raised to  $\phi_0$  above that of the membrane. Our problem is to determine for arbitrary choice of the geometrical ratios  $H/R$  and  $X/R$ : (i) the range of values of  $\phi_0$  for which an equilibrium configuration is possible, and (ii) the profile of the membrane in its equilibrium configuration.

Let us suppose that an equilibrium configuration exists for a given value of  $\phi_0$ . The equations which must be satisfied are that:

(1) The electrostatic potential  $\phi$  satisfies  $\nabla^2\phi = 0$  in the non-conducting region bounded by the cylinder, the membrane and the rigid half planes.

(2)  $\phi = \phi_0$  on the cylinder.

(3)  $\phi = 0$  on the membrane and rigid half planes.

(4) The normal stress condition on the membrane must be satisfied. Let  $T$  denote the surface tension on each side of the membrane and  $K$  denote the dielectric constant in the non-conducting region, then the normal stress condition can be written as

$$\frac{T}{\rho} + \frac{K}{16\pi} \left[ \frac{\partial\phi}{\partial n} \right]^2 = 0 \quad (|x| < X), \quad (37)$$

where  $\rho$  denotes the algebraic radius of curvature (i.e. the inverse of the curvature) and  $n$  measures distance along the normal at any point of the membrane into the non-conducting region. On making  $\rho$ ,  $n$ ,  $x$ ,  $X$  and  $\phi$  dimensionless using  $R$  and  $\phi_0$  for the reference length and potential respectively, equation (37) becomes

$$\frac{1}{\rho} + \frac{1}{2}\mu^2 \left[ \frac{\partial\phi}{\partial n} \right]^2 = 0 \quad (|x| < X), \quad (38)$$

where  $\mu^2 = K\phi_0^2/8\pi TR$ .

In order to obtain a solution of the problem posed by (1) to (4) above, we have found it advantageous to work in bipolar coordinates rather than Cartesian coordinates. The relations between the Cartesian coordinates  $(x, y)$  and the bipolar coordinates  $(\xi, \eta)$  are

$$x = \frac{c \sin \eta}{\cosh \xi - \cos \eta}, \quad y = \frac{c \sinh \xi}{\cosh \xi - \cos \eta} \quad (-\pi < \eta \leq \pi). \quad (39)$$

The *cylinder* is given by  $\xi = \alpha$  ( $\alpha > 0$ ) and the *plane*  $y = 0$  by  $\xi = 0$ , with  $H = \cosh \alpha$  and the constant  $c$  appearing in (39) is given by  $c = \sinh \alpha$ . The equation of the membrane is now  $\xi = Y(\eta)$  with  $\eta_X \leq \eta \leq \pi$  and  $-\eta_X \geq \eta > -\pi$ , where  $Y(\eta)$  is a function to be determined and  $(0, \eta_X)$  and  $(0, -\eta_X)$  denote the bipolar coordinates of the edges of the membrane. It therefore immediately follows from (39) that

$$\frac{X}{c} = \frac{\sin \eta_X}{1 - \cos \eta_X} = \cot \left( \frac{1}{2}\eta_X \right), \quad (40)$$

which gives  $\eta_X = 2 \cot^{-1}(X/c) = 2 \cot^{-1}(X/\sqrt{H^2 - 1})$ . The conducting half planes will be given by  $\xi = 0$  ( $\eta < \eta_X$ ). We can observe from (38) that the membrane must always be convex towards the cylinder, thus  $Y(\eta) \geq 0$ .

Bipolar coordinates form an orthogonal curvilinear coordinate system, as demonstrated in Morse & Feshbach (1953) for example, and the linear element scales  $h_1$  and  $h_2$  are given by

$$h_1 = h_2 = c(\cosh \xi - \cos \eta)^{-1},$$

from which it follows that

$$\nabla^2\phi = \frac{(\cosh \xi - \cos \eta)^2}{c^2} \left[ \frac{\partial^2\phi}{\partial \xi^2} + \frac{\partial^2\phi}{\partial \eta^2} \right], \quad (41)$$

$$\left[ \frac{\partial\phi}{\partial n} \right]_{\xi=Y}^2 = \frac{(\cosh Y - \cos \eta)^2}{c^2} \left[ \left( \frac{\partial\phi}{\partial \xi} \right)^2 + \left( \frac{\partial\phi}{\partial \eta} \right)^2 \right]_{\xi=Y}. \quad (42)$$

In order to simplify setting up the numerical computation procedure for determining  $\phi$ , it is convenient to introduce the auxiliary coordinates  $\zeta, \theta$  defined by

$$\zeta = \alpha - \xi, \quad \theta = \pi - \eta.$$

The cylinder will now be given by  $\zeta = 0$  and the membrane-plane surface by  $\zeta = \alpha - Y$ , where  $Y = 0$  for  $|\theta| < \theta_x$  with  $\theta_x = 2 \tan^{-1}(X/c)$ . Because of the symmetry of the problem it is clear that we need only consider values of  $\theta$  for which  $0 \leq \theta \leq \pi$ . The problem for determining the solution of Laplace's equation in the  $(\zeta, \theta)$  plane is represented diagrammatically in figure 11, where of course the curved part of the boundary is one of the unknowns of the problem.

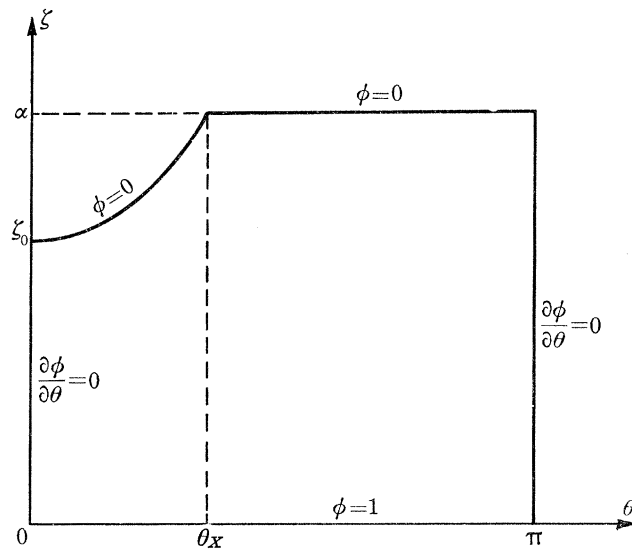


FIGURE 11. The domain of the problem for determining  $\phi$  in the  $(\zeta, \theta)$  plane.

In order to express the normal stress condition (38) in terms of bipolar coordinates, we need to derive the appropriate expression for the radius of curvature  $\rho$ . In Cartesian coordinates we have

$$\frac{1}{\rho} = \frac{d^2y}{dx^2} \left[ 1 + \left( \frac{dy}{dx} \right)^2 \right]^{-\frac{3}{2}},$$

and the surface of the membrane is given by

$$\frac{x}{c} = \frac{\sin \eta}{\cosh Y - \cos \eta}, \quad \frac{y}{c} = \frac{\sinh Y}{\cosh Y - \cos \eta} \quad (\eta_x \leq \eta \leq \pi), \quad (43)$$

where  $Y = Y(\eta)$ . After some algebraic manipulation it may be verified that

$$c \frac{d^2y}{dx^2} = \frac{(\cosh Y - \cos \eta)^4}{(1 - \cosh Y \cos \eta)^3 (\sin \eta Y' - \sinh Y)^3} \left\{ Y'' - \frac{[\sin \eta Y' - \sinh Y][1 + (Y')^2]}{\cosh Y - \cos \eta} \right\}, \quad (44)$$

$$1 + \left( \frac{dy}{dx} \right)^2 = \frac{(\cosh Y - \cos \eta)^2 [1 + (Y')^2]}{(1 - \cosh Y \cos \eta)^2 (\sin \eta Y' - \sinh Y)^2}, \quad (45)$$

where the prime denotes  $d/d\eta$ . It follows immediately from (44) and (45) that

$$\frac{c}{\rho} = \frac{\cosh Y - \cos \eta}{[1 + (Y')^2]^{\frac{3}{2}}} \left\{ Y'' - \frac{[\sin \eta Y' - \sinh Y][1 + (Y')^2]}{\cosh Y - \cos \eta} \right\}. \quad (46)$$

If we now replace the coordinate  $\eta$  by the auxiliary coordinate  $\theta$ , it then follows that the normal stress condition (38) when expressed in terms of the coordinates  $(\xi, \theta)$  has the form:

$$Y'' = -\frac{[Y' \sin \theta + \sinh Y][1 + (Y')^2]}{(\cosh Y + \cos \theta)} - \frac{\mu^2}{2c} (\cosh Y + \cos \theta) [1 + (Y')^2]^{\frac{3}{2}} \left[ \left( \frac{\partial \phi}{\partial \xi} \right)^2 + \left( \frac{\partial \phi}{\partial \theta} \right)^2 \right]_{\xi=Y}, \quad (47)$$

where the prime now denotes differentiation with respect to  $\theta$ .

The asymptotic form of the solution of (47) when  $\mu \ll 1$  may be developed by looking for expansions of  $Y(\theta)$  and  $\phi(\xi, \theta)$  of the form

$$\begin{aligned} Y(\theta) &= \mu^2 Y_1(\theta) + \mu^4 Y_2(\theta) + \dots, \\ \phi(\xi, \theta) &= \phi_0(\xi, \theta) + \mu^2 \phi_1(\xi, \theta) + \dots \end{aligned}$$

Clearly  $\phi_0$  would be the solution for  $\phi$  appropriate when the membrane is plane and is thus  $\phi_0(\xi, \theta) = \xi/\alpha$ . Consequently,

$$\left[ \left( \frac{\partial \phi_0}{\partial \xi} \right)^2 + \left( \frac{\partial \phi_0}{\partial \theta} \right)^2 \right]_{\xi=0} = \frac{1}{\alpha^2},$$

and the differential equation for  $Y_1(\theta)$  is

$$(1 + \cos \theta) Y_1'' + Y_1' \sin \theta + Y_1 = -(2c\alpha^2)^{-1} (1 + \cos \theta)^2, \quad (48)$$

the boundary conditions being  $Y'(0) = 0$ ,  $Y_1(\theta_X) = 0$ . The solution of (48) satisfying these boundary conditions is

$$Y_1 = \frac{1}{2c\alpha^2} \left\{ \frac{\theta_X \sin \theta_X}{1 + \cos \theta_X} - \frac{\theta \sin \theta}{1 + \cos \theta} \right\} (1 + \cos \theta).$$

Thus to the first order in  $\mu^2$ , the solution of (47) when  $\mu \ll 1$  is

$$Y = (\mu^2/2\alpha^2 \sinh \alpha) [\theta_X \tan \frac{1}{2}\theta_X - \theta \tan \frac{1}{2}\theta] (1 + \cos \theta). \quad (49)$$

This form of linear solution assumes that  $\mu^2 \ll \alpha^2 \sinh \alpha$  which implies that the clearance between the cylinder and the membrane is on the length scale of the radius of the cylinder. The case when  $\alpha^3 \approx \mu^2 \ll 1$  corresponds to the geometrical configuration discussed in § 2 where we have shown that  $\beta$ , and therefore  $\mu$ , must lie below a certain value for equilibrium to be possible. The solution (49) gives no indication of the existence of a restriction on the permissible values of  $\mu$  for equilibrium in the general case and for such information we must examine the full nonlinear problem. Since both the electrostatic potential function and part of the boundary of the region over which it is defined are unknowns, to determine the range of values of  $\mu$  for which equilibrium is possible when we place no restrictions on the geometrical parameters is a problem of some complexity and we have approached it by the use of numerical techniques.

#### *The numerical solution*

The equilibrium shape of the membrane, if it exists, for a given value of  $\mu$  and given geometrical parameters  $H$  and  $X$  is determined numerically by iteration. We first assume a trial equilibrium shape for the membrane and then (A) solve Laplace's equation for  $\phi$  in the region bounded by the cylinder, the membrane and the conducting half planes and from this solution compute the electrostatic stress over the membrane. This is then used for the computation of the term

$$\left[ \left( \frac{\partial \phi}{\partial \xi} \right)^2 + \left( \frac{\partial \phi}{\partial \theta} \right)^2 \right]_{\xi=Y},$$

which appears in (47). We are then in a position to (B) proceed to integrate equation (47) and so determine a 'new' equilibrium shape for the membrane. We can then repeat procedures (A) and (B) until successive approximations to the membrane shape agree to a prescribed degree of accuracy. For a small value of  $\mu$ , the linear solution (49) may be used to give the initial trial value for the membrane shape and when a true equilibrium shape has been determined for that value of  $\mu$ , this solution can be used for the initial shape for a slightly larger value of  $\mu$ . In this way we can increase  $\mu$  to determine the maximum value  $\mu_c$  for which the membrane can be in stable equilibrium for the given geometry defined by the choice of  $H/R$  and  $X/R$ . As  $\mu \rightarrow \mu_c$ , we find that the number of iterations increases and when  $\mu > \mu_c$  the procedures (A) and (B) fail to produce a convergent solution. The maximum elevation of each 'new' shape increases until it exceeds  $(H-1)$  and this provides us with a useful cut-off criterion for terminating the computer program.

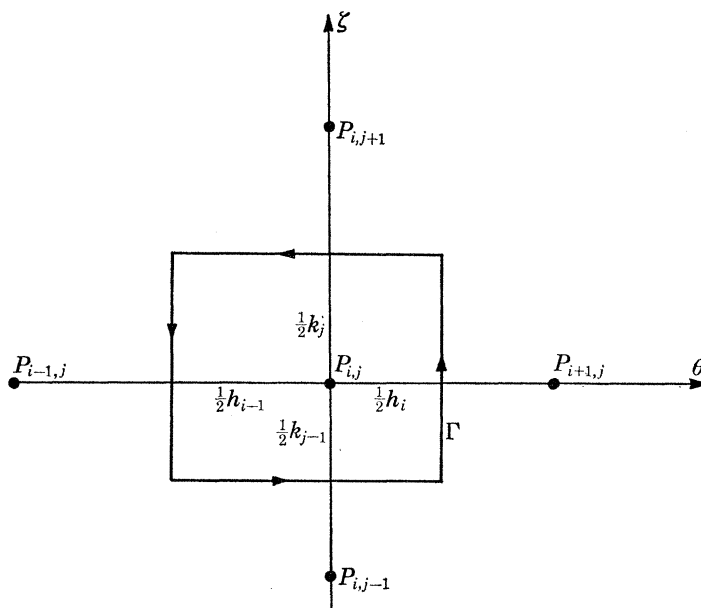


FIGURE 12. The grid network at a typical grid point  $P_{i,j}$ .

The grid network to cover the domain of  $\phi$  in the  $(\zeta, \theta)$  plane (see figure 11) was fixed in the following manner. The interval  $(0, \theta_x)$  was divided into  $N$  equal subintervals,  $(\theta_x, \pi)$  into  $(N_1 - N)$  equal subintervals and  $(0, \zeta_0)$  into  $M$  equal subintervals. The grid lines parallel to the  $\theta$ -axis for  $\zeta_0 < \zeta \leq \alpha$  were determined by choosing as grid points the intersections of the grid lines parallel to the  $\zeta$ -axis for  $0 \leq \theta \leq \theta_x$  with the membrane. With the independent choice of  $N$ ,  $N_1$  and  $M$ , this grid structure permitted us to construct small grid cells in the region of the domain where the cylinder and membrane are closest while at the same time use larger cells for the region where the solution would not be expected to deviate much from that for a plane membrane. The values of  $\phi$  at grid points other than those on the cylinder, membrane and planes were computed by means of a second-order difference equation at each grid point. This difference equation was derived in the following way. Figure 12 shows a typical group of five neighbouring grid points. The rectangle  $\Gamma$  forms the midpoints of  $P_{i,j}$ ,  $P_{i+1,j}$ , etc. Because  $\phi$  is a harmonic function it follows that

$$\int_{\Gamma} \frac{\partial \phi}{\partial n} ds = 0,$$

from which we deduce the approximate formula

$$A_{i,j}\phi_{i,j} + B_{i,j}\phi_{i-1,j} + C_{i,j}\phi_{i+1,j} + D_{i,j}\phi_{i,j-1} + E_{i,j}\phi_{i,j+1} = 0, \quad (50)$$

where  $\phi_{i,j} = \phi(P_{i,j})$  and

$$\begin{aligned} -B_{i,j} &= (k_{j-1} + k_j)h_{i-1}, & -C_{i,j} &= (k_{j-1} + k_j)h_i, \\ -D_{i,j} &= (h_{i-1} + h_i)k_{j-1}, & -E_{i,j} &= (h_{i-1} + h_i)k_j, \\ -A_{i,j} &= B_{i,j} + C_{i,j} + D_{i,j} + E_{i,j}. \end{aligned}$$

It will be seen that the above formulation is valid at all grid points, including those adjacent to grid points on the membrane and at grid points where adjacent subinterval lengths either in the  $\theta$  or  $\zeta$  directions (or both) are different. For grid points on  $\theta = 0$  or  $\theta = \pi$  we use the symmetry condition that

$$\phi_{i-1,j} = \phi_{i+1,j}.$$

The set of linear equations for  $\phi_{i,j}$  has a band structured matrix which means that it is relatively simple to handle a large number of grid points; in fact in our calculations we worked with up to 875 grid points at which the value of  $\phi$  is to be determined and solved the resulting set of linear equations by Gaussian elimination. When the values of  $\phi_{i,j}$  are known, the reduced normal stress on the membrane due to the electrostatic field

$$\left[ \left( \frac{\partial \phi}{\partial \zeta} \right)^2 + \left( \frac{\partial \phi}{\partial \theta} \right)^2 \right]_{\zeta=\alpha-Y}$$

is determined from the numerical solution at the grid points on the membrane and also at the mid-way points by quadratic interpolation. These values are then used in the integration of (47). This equation may be written as

$$Y'' = f(\theta, Y, Y')$$

with the boundary conditions  $Y'(0) = 0$ ,  $Y(\theta_X) = 0$ . The complexity of this nonlinear differential equation makes an orthodox approach to this two point boundary-value problem complicated and tedious. We therefore decided to treat the problem as an initial-value problem, prescribing a value of  $Y(0)$  and going on to compute the solution using a fourth-order Runge-Kutta procedure. If the boundary condition at  $\theta = \theta_X$  were not satisfied to a specified degree of accuracy, the value of  $Y(0)$  would be altered and the integration performed again. Further refinement of the value of  $Y(0)$  was then effected by a linear interpolation-extrapolation formula relating  $Y(0)$  to  $Y(\theta_X)$  so as to determine the choice of  $Y(0)$  to obtain satisfaction of the boundary condition at  $\theta = \theta_X$ .

The accuracy to which the critical values  $\mu_c$  can be evaluated by this general numerical procedure is naturally limited by the number of grid points which are used in discretizing the domain of definition of  $\phi$  in the  $(\zeta, \theta)$  plane. The number of grid points is in turn limited by the storage capacity of the computer used for the calculations. Some of the early calculations were carried out on the IBM-360 computer at University College London, but the bulk of the computation was effected on the UNIVAC 1108 at Carnegie-Mellon University. The mode in which both of these machines are operated places a restriction on the number of grid points which can be used but we have found that by choosing

$$M = 16, \quad N = 11, \quad N_1 = 21,$$

the storage required is just within either machine's capability using double precision arithmetic and we have been able to obtain a good representation of both the solution of Laplace's equation in the  $(\zeta, \theta)$  plane and the elevation of the membrane. The complexity of the problem prevents us from giving a precise estimate of the errors arising from any prescribed choice of discretization.



A crude estimate of the errors in both the solution of Laplace's equation and the integration of the differential equation representing the normal stress condition may of course be made in the usual way. However, (a) the agreement between calculations of  $\mu_c$  and calculations of  $\beta_c$  in those geometrical configurations where comparison is possible, and (b) the calculations of some check values with each of  $M$ ,  $N$  and  $N_1$  increased by 5 which were carried out on the IBM 360 machine at Carnegie-Mellon University operating on a time-sharing system and offering a vastly increased storage capability, has led us to believe that the method will give  $\mu_c$  with the stated choice of grid network to an accuracy of at least two significant figures for all values of the geometrical parameters considered.

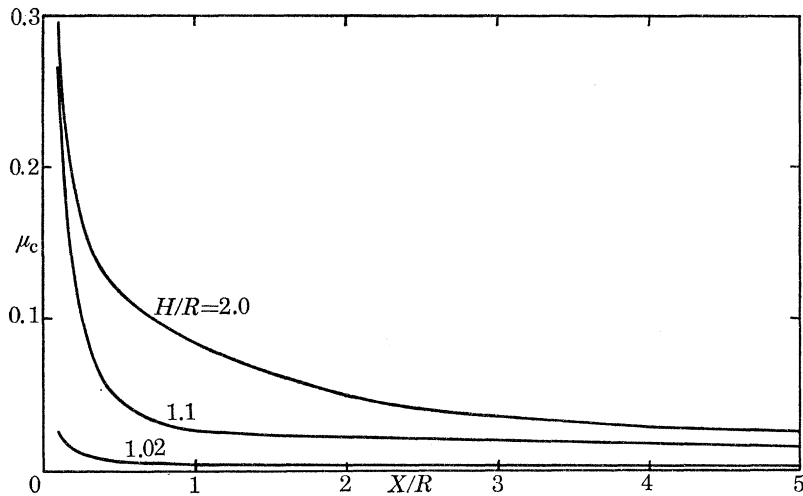


FIGURE 13. The variation of  $\mu_c$  with  $X/R$  for fixed values of  $H/R$ . The value of  $10^{-1}\mu_c$  is plotted for  $H/R = 2.0$ .

For a given choice of  $M$ ,  $N$  and  $N_1$  the number of grid points at which the value of  $\phi$  is to be determined is  $L_s$  where

$$L_s = N(M-1) + \frac{1}{2}N(N-1) + (N_1 - N)(M + N - 2).$$

The number  $L_s$  is therefore the total number of linear equations which must be solved for the unknown  $\phi_{i,j}$ . The corresponding number of elements of the matrix of coefficients in this set of equations, excluding the zero elements below the lower diagonal and above the upper diagonal bounding the band is  $L_A$  where

$$L_A = L_s(2M + 2N - 3) - (M + N - 2)(M + N - 1).$$

In the case when  $M = 16$ ,  $N = 11$ ,  $N_1 = 21$ , we have  $L_s = 470$  and  $L_A = 23640$ .

In figure 13 the values of  $\mu_c$  for the fixed values of  $H/R = 1.02$ ,  $1.1$  and  $2.0$  are plotted as a function of  $X/R$  with  $X/R$  taking values from  $0.1$  to  $5.0$ . In order to fit the three curves in the same diagram we have plotted  $10^{-1}\mu_c$  for the case when  $H/R = 2.0$ . It will be seen that the range of values of  $\mu$  for which the membrane can be in an equilibrium configuration decreases rapidly as the width of the membrane increases.

In figure 14 the profiles of the semi-membrane for the stable equilibrium configurations are drawn for  $H/R = 1.75$  and  $X/R = 5.0$  with  $\mu$  increasing from zero to its critical value  $\mu_c = 0.2$ . These profiles are drawn to the same scale so that the changes in shape of the membrane may be observed as  $\mu$  is increased. The elevation remains quite small until  $\mu$  approaches  $\mu_c$ . We find that

the elevation of the centre of the membrane is less than 14 % of the gap until  $\mu$  exceeds 0.15. The distortion of the membrane from its original plane form then becomes very rapid with an elevation of the centre equal to  $0.304R$ , or more than 40 % of the gap when  $\mu = \mu_c$ . It can be seen that the membrane becomes more angular and pointed at the centre as the critical value of  $\mu$  is reached, so that the curvature becomes essentially non-zero only near the centre, indicating that the electrostatic stress and therefore the charge density becomes small at all points of the membrane other than in the neighbourhood of the centre.

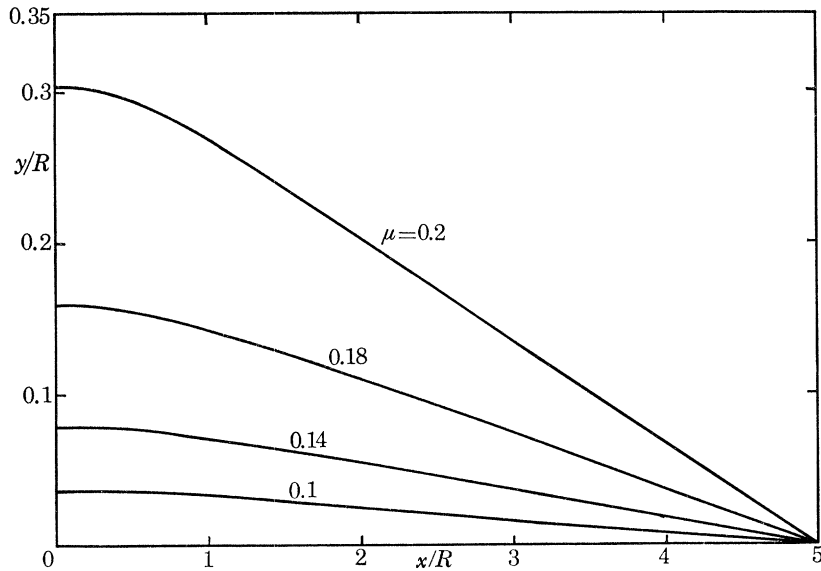


FIGURE 14. The profiles of the equilibrium shape of the membrane for values of  $\mu$  increasing to  $\mu_c = 0.2$  for  $H/R = 1.75$  and  $X/R = 5.0$ .

The curves displayed in figure 14 typify the changes in the shape of the profiles that are observed for other values of  $H/R$  and  $X/R$  which we considered and a similar pattern of distortion of the membrane occurs if the profiles at the critical  $\mu$  are drawn for fixed  $X/R$  but varying  $H/R$ , the angular shape being more pronounced at a larger gap distance.

*A comparison between results from the exact and asymptotic theories*

We now return to the problem (d) of § 2 where a rigid conducting circular cylinder is placed near a conducting membrane which is assumed to be plane in the absence of any electric field. The conditions of that problem can be closely simulated in the general problem which we have discussed in this section if we choose the geometrical parameters  $H$  and  $X$  so that

$$(H-R)/R \ll X/R \ll 1.$$

In table 4 we set out the results of calculating  $\mu_c$  from the exact equations and  $\bar{\mu}_c$  from the asymptotic theory of § 1. For the comparison we chose  $H/R = 1.02, 1.1$  and  $2.0$  with  $X/R = 0.1, 0.2, 0.2582, 0.4, 0.6, 1.0$  and  $2.0$ . Apart from the choice of  $X/R = 1.0$ , and  $2.0$ , with  $H/R = 2.0$  the values chosen for the parameters may be regarded as loosely satisfying the requirements for the asymptotic theory to be valid. Referring to figures 5 and 10 we see that the relations between the parameters used to describe the geometrical configurations for the two theories are given by

$$\sigma = X/a_1, \quad H-R = 2h - a_1^2/2R,$$

if we identify  $X$  with  $a_2$ . It therefore follows that

$$\alpha^* = \left( \frac{1}{2} + \frac{(H-R)R\sigma^2}{X^2} \right)^{-1}.$$

The relation between  $\beta$  and  $\mu$  can immediately be deduced by setting  $\phi_0 = 2V_0$  and noting that in the definition of  $\beta$  given in (d) of § 2, the surface tension must be doubled for a membrane. We therefore have

$$\mu^2 = \frac{2\beta\sigma^2 R^2}{X^2} \left( \frac{H}{R} - 1 + \frac{X^2}{2\sigma^2 R^2} \right)^3.$$

The choice of the parameter  $\sigma$  is restricted since for the asymptotic theory of § 1 to be valid,

$$h \ll a_1 = X/\sigma.$$

TABLE 4

$H/R$	$X/R$	$\mu_c$	$\bar{\mu}_c(1)$	$\bar{\mu}_c(2)$	$\bar{\mu}_c(3)$
1.02	0.1	0.025	0.0249	0.0272	0.0307
	0.2	0.014	0.0136	0.0144	0.0159
	0.2582	0.011	0.0111	0.0116	0.0126
	0.4	0.008	0.0082	0.0083	0.0088
	0.6	0.006	0.0063	0.0063	0.0065
	1.0	0.004	0.0047	0.0047	0.0047
	2.0	0.003	—	0.0039	0.0040
1.1	0.1	0.267	0.2669	0.2962	0.3374
	0.2	0.136	0.1369	0.1501	0.1699
	0.2582	0.106	0.1082	0.1176	0.1324
	0.4	0.059	0.0740	0.0787	0.0872
	0.6	0.038	0.0538	0.0559	0.0605
	1.0	0.027	0.0377	0.0383	0.0399
	2.0	0.024	—	0.0367	0.0373
2.0	0.1	2.95	8.372	9.325	10.647
	0.2	1.94	4.198	4.669	5.327
	0.2582	1.64	3.260	3.621	4.129
	0.4	1.30	2.122	2.348	2.671
	0.6	1.11	1.839	1.920	2.089
	1.0	0.862	1.207	1.298	1.457
	2.0	0.495	—	0.8357	0.9276

For our calculations we chose  $\sigma = 1, 2, 3$  for the values of  $X/R \leq 1.0$ . When  $X/R = 2.0$  there is no corresponding asymptotic solution for  $\sigma = 1$ . The results of the calculations of  $\mu$  which were carried out by means of the asymptotic theory are tabulated as  $\bar{\mu}_c(\sigma)$  in table 4. It will be seen that there is a very good measure of agreement between  $\bar{\mu}_c(\sigma)$  and  $\bar{\mu}_c$  for those values of  $H/R$ ,  $X/R$  and  $\sigma$  which come closest to satisfying the restrictions on the geometrical parameters for the asymptotic theory to be valid. In the case when  $H/R = 1.02$ , the relative error between the asymptotic and the numerical solutions is less than 5% for  $X/R < 0.6$  when  $\sigma = 1$ . The error exceeds 14% when  $X/R = 1.0$  and when  $X/R = 2.0$  the error is now 30% with  $\sigma = 2$ , the value of  $\bar{\mu}_c(1)$  does not now exist. When  $H/R = 1.1$ , the relative error is better than 2% for  $X/R \leq 0.2582$  with  $\sigma = 1$ . The error increases rapidly as  $X/R$  increases, it being 20% when  $X/R = 0.4$  and about 50% when  $X/R = 2.0$ , again choosing the most favourable value of  $\bar{\mu}_c(\sigma)$  in each case to make the comparison with  $\mu_c$ . When  $H/R = 2.0$ , as expected the tabulation shows a wide divergence between the two theories over all values of  $X/R$  and  $\sigma$  indicating that the asymptotic theory cannot now provide any useful information in such geometrical configurations. The apparently better agreement between the asymptotic and exact theories for  $H/R = 1.1$  when compared with

$H/R = 1.02$  is probably due to the lack of significance which can be achieved from the numerical solution with the grid mesh size used when the gap between the conductors is very small. In this situation the asymptotic theory provides the better method for determining  $\mu_c$ .

It will be further noticed from table 4 that the values of  $\bar{\mu}_c(\sigma)$  are more sensitive to the choice of  $\sigma$  when  $X/R$  is small. This reflects the effect of the assumptions we have made in deriving the boundary condition at  $x = 1$  and the solution for the electrostatic potential for  $1 \leq x \leq \sigma$  in the analysis of § 2(d). It is therefore evident that in those geometrical configurations where the asymptotic theory is accurate, it is essential that the presence of the solid conductor should be taken into account for  $|x| \leq X$ .

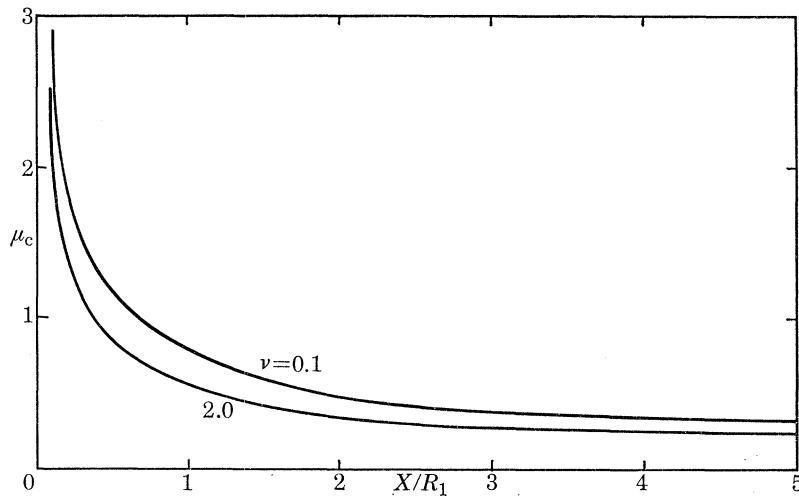


FIGURE 15. Variation of  $\mu_c$  with  $X/R_1$  for  $H/R_1 = 2.0$  with  $\nu = 0.1, 2.0$ .

#### *Some related problems*

In the preceding discussion we have assumed that in the absence of the electric field the membrane is plane and consequently there is zero pressure difference across the membrane. In the case where the pressure on the cylinder side of the membrane is  $p$  say above that on the other side, the equilibrium shape for the membrane in the absence of the electric field will be an arc of circle of radius  $R_2$  where  $R_2 = 2T/p$ . The modified dimensionless form of the normal stress condition when the membrane is in equilibrium under the influence of the electric field is now

$$\frac{1}{\rho} + \frac{\mu^2}{2} \left[ \frac{\partial \phi}{\partial n} \right]^2 + \nu = 0 \quad (|x| < X), \quad (51)$$

where  $\nu = pR_1/2T = R_1/R_2$ . This equation written in terms of the coordinates  $(Y, \theta)$  becomes

$$Y'' = - \frac{Y' \sin \theta + \sinh Y [1 + (Y')^2]}{\cosh Y + \cos \theta} - \frac{\mu^2}{2c} (\cosh Y + \cos \theta) [1 + (Y')^2]^{\frac{3}{2}} \left[ \left( \frac{\partial \phi}{\partial \xi} \right)^2 + \left( \frac{\partial \phi}{\partial \theta} \right)^2 \right]_{\xi=Y} - \frac{\nu [1 + (Y')^2]^{\frac{3}{2}}}{c \cosh Y + \cos \theta} \quad (0 \leq \theta \leq \pi). \quad (52)$$

The solution of this problem may be determined using the numerical techniques described at length earlier, the only change necessary is that the additional term appearing in equation (52) must be included. We have carried out calculations of  $\mu_c$  for a fixed value of  $H/R_1 = 2.0$  for  $\nu = 0.1$  and  $\nu = 2.0$ , where  $R_1$  denotes the radius of the solid conductor. The results of these calculations are displayed in figure 15.

When  $H/R_1 \approx 1$ , we can perform computations so as to compare with corresponding results derived from the asymptotic theory of § 2(d) with  $\alpha_2 \neq 0$ . The expression for  $\alpha_1$  in terms of  $H, X, R_1$  and  $\sigma$  is the same as that given for  $\alpha$  when  $\nu = 0$  with  $R_1$  replacing  $R$ . From the definitions of  $\alpha_1$  and  $\alpha_2$  given in § 2(d) and the definition of  $\nu$  given above, it follows that  $\alpha_2 = \nu\alpha_1$ .

From figure 5, it will be seen that when  $\mu = 0$  there is a geometrical constraint which requires that

$$R_1 + R_2 \leq H + (R_2^2 - a_2^2)^{\frac{1}{2}},$$

where  $H$  denotes the distance of the centre of the conducting cylinder from the plane  $y = 0$ . This constraint means that the choice of  $\nu, H, X$  and  $R_1$  must be such that

$$1 + \frac{1}{\nu} \leq \frac{H}{R_1} + \left( \frac{1}{\nu^2} - \frac{X^2}{R_1^2} \right)^{\frac{1}{2}}.$$

Comparative results from the numerical and asymptotic solutions are shown in table 5 for  $H/R_1 = 1.04$  and  $\nu = 0.02$ . We again adopt the convention of denoting asymptotic values of  $\mu_c$  by  $\bar{\mu}_c(\sigma)$ .

TABLE 5

$X/R_1$	$\mu_c$	$\bar{\mu}_c(1)$	$\bar{\mu}_c(2)$	$\bar{\mu}_c(3)$
0.1	0.036	0.0361	0.0389	0.0436
0.2	0.25	0.0258	0.0272	0.0298
0.3	0.016	0.0177	0.0181	0.0192
0.5	0.009	0.0113	0.0114	0.0116

It will be observed that there is good agreement between the results derived from the two solutions for this choice of  $H/R_1$  when  $X/R_1 = 0.1$  or  $0.2$  and  $\sigma = 1$ , the relative error being less than 4% for these cases. However, with increasing  $X/R_1$  the divergence of results becomes more pronounced than for the corresponding geometrical configuration with  $\nu = 0$ . At  $X/R_1 = 0.3$  the relative error is about 12% while for  $X/R_1 = 0.5$  the relative error is in excess of 22%.

Because of the nature of bipolar coordinates in that both the circular cylinder and the plane  $y = 0$  transform into planes in the  $(\xi, \eta, z)$  space, it is a simple matter to derive the equations for solving the dual problem of a long cylindrical filament of conducting fluid which in the absence of the electric field is at rest parallel to a conducting rigid plane. However, even if the filament is neutrally buoyant in the dielectric medium surrounding it, when there is a potential difference between the filament and the plane, the filament experiences a net force towards the plane and cannot therefore remain in equilibrium. A modified form of the theory of this section could nevertheless be used to study the instantaneous change of shape of the filament as it moves towards the plane.

In conclusion we may point out that there is no difficulty in principle which prevents us from adapting the numerical procedures discussed in this section so that the solutions of analogous problems in three dimensions with axial symmetry can be determined.

The authors are most grateful for the assistance of Miss S. M. Burrough with much of the computational work of §§ 1 and 2 and also for the computing facilities which were made available to us by Carnegie-Mellon University and University College London. The work described in this paper was completed while one of us (M. E. O'N.) was a visiting member of faculty in the Department of Chemical Engineering, Carnegie-Mellon University, and during this time he was supported in a fellowship of Mellon Institute by the American Iron and Steel Institute.

## REFERENCES

- Ackerberg, A. 1969 *Proc. R. Soc. Lond. A* **312**, 129.  
Allan, R. S. & Mason, S. G. 1961 *Trans. Faraday Soc.* **57**, 2027.  
Allan, R. S. & Mason, S. G. 1962 *J. Colloid Sci.* **17**, 383.  
Jayaratne, O. W. & Mason, B. J. 1964 *Proc. R. Soc. Lond. A* **280**, 545.  
Latham, J. & Roxburgh, I. W. 1966 *Proc. R. Soc. Lond. A* **295**, 84.  
Morse, P. M. & Feshbach, H. 1953 *Methods of theoretical physics*, vol. I. New York: McGraw-Hill.  
Rayleigh, Lord 1882 *Phil. Mag.* **14**, 184.  
Taylor, G. I. 1964 *Proc. R. Soc. Lond. A* **280**, 383.  
Taylor Sir Geoffrey 1968 *Proc. R. Soc. Lond. A* **306**, 423.  
Thompson, J. M. T. 1963 *J. Mech. Phys. Solids* **11**, 13.